Fraunhofer Institut
Techno- und
Wirtschaftsmathematik

Interval Methods for Analog Circuits

Dr. Alexander Dreyer

Abstract

Reliable methods for the analysis of tolerance-affected analog circuits are of great importance in nowadays microelectronics. It is impossible to produce circuits with exactly those parameter specifications proposed in the design process. Such component tolerances will always lead to small variations of a circuit's properties, which may result in unexpected behaviour. If lower and upper bounds to parameter variations can be read off the manufacturing process, interval arithmetic naturally enters the circuit analysis area.

This paper focuses on the frequency-response analysis of linear analog circuits, typically consisting of current and voltage sources as well as resistors, capacitances, inductances, and several variants of controlled sources. These kind of circuits are still widely used in analog circuit design as equivalent circuit diagrams for representing in certain application tasks

Interval methods have been applied to analog circuits before. But yet this was restricted to circuit equations only, with no interdependencies between the matrix elements. But there also exist formulations of analog circuit equations containing dependent terms. Hence, for an efficient application of interval methods, it is crucial to regard possible dependencies in circuit equations. Part and parcel of this strategy is the handling of fill-in patterns for those parameters related to uncertain components. These patterns are used in linear circuit analysis for efficient equation setup. Such systems can efficiently be solved by successive application of the *Sherman-Morrison formula*.

The approach can also be extended to complex-valued systems from frequency domain analysis of more general linear circuits. Complex values result here from a Laplace transform of frequency-dependent components like capacitances and inductances. In order to apply interval techniques, a real representation of the linear system of equations can be used for separate treatment of real and imaginary part of the variables. In this representation each parameter corresponds to the superposition of two fill-in patterns. Crude bounds – obtained by treating both patterns independently – can be improved by consideration of the correlations to tighter enclosures of the solution.

The techniques described above have been implemented as an extension to the toolbox *Analog Insydes*, an add-on package to the computer algebra system *Mathematica* for modeling, analysis, and design of analog circuits.

Keywords: interval arithmetic, analog circuits, tolerance analysis, parametric linear systems, frequency response, symbolic analysis, CAD, computer algebra

1 Motivation

Numerical simulations of analog circuits can be used to analyze a circuit's behaviour without the need for a physical implementation. But actual circuit properties may differ from the results obtained by floating-point simulations, due to errors caused by rounding, component tolerances, and simplified models. Simulations based on interval arithmetic can be used as a unified framework to bound all these errors, but tend to be too conservative. In this paper a new approach for computing tight bounds to the frequency response of tolerance-affected analog circuits is described.

The behaviour of analog circuits can be described by a system of parameter-dependent linear or nonlinear equations. A symbolic setup of the equation system allows for assigning unique symbols to each circuit component parameter. The resulting circuit equations however often cannot be analyzed in a pure symbolic way: In the nonlinear case the system might not be solvable in a symbolic manner, but yet in the linear case the result may be of large complexity. In order to analyze the behaviour of such an analog circuit using a simulator or a numerical solver, the symbols representing netlist elements have to be replaced by the corresponding numerical values, according to a given design point.

The numerical approach has two major drawbacks: First of all, for an efficient numerical treatment of the equation system, all numerical values have to be converted into floating-point numbers. This may lead to growing of the overall error, due to rounding of the numerical values in each solving step. Another problem is caused by the fact that a design point may be defined in advance, but one cannot ensure a priori that the desired properties will exactly be met during manufacturing of the actual circuit. Component tolerances will always lead to small variations of a circuit's properties, which may result in effects not expected from the results of the numerical simulation. While rounding errors could be reduced or even completely avoided by a sophisticated treatment of the equation system, the latter problem cannot be overcome within a single numerical simulation. Using a statistical method, like the Monte Carlo approach, the parameter variations of the production process may be simulated [1]. But this results in a large number of simulations and does not yield guaranteed solutions. Simulation based on *interval arithmetic* can be used as a unified framework for both problems.

This paper starts with a brief introduction to the principles of interval computations and the relevance of interdependences to the accuracy of interval-valued results. Then mathematical methods especially tuned to handle systems arising from frequency-response analysis of linear analog circuits are described. This includes an approach, which is capable of computing tight bounds to variations due to a large number of tolerance-affected components. Finally, the results are illustrated on several an example applications.

2 Interval Arithmetic

2.1 Basics

If upper and lower bounds for the uncertain parameters can be determined, these can be interpreted as the endpoints $\underline{x}$, $\overline{x}$ of a closed interval $[\underline{x}, \overline{x}] \subseteq \mathbb{R}$. This interval is usually denoted by $[x]$. A vector of intervals – or *box* – is consequently written as $[\mathbf{x}]$. The principles of interval arithmetic are quite simple (e.g. [2, 3]): during evaluation any expression is constructed by subsequent calls of elementary binary operations $(+, -, *, /)$ and basic functions like *sin*, *cos*, *log*, e^x and x^n, where the *intervalization* of binary operators is

$$\begin{aligned} [\underline{x}, \overline{x}] \diamond [\underline{y}, \overline{y}] &= [\underline{z}, \overline{z}], \text{ for } \diamond \in \{+, -, *, /\}\,, \\ \text{with } \underline{z} &= \min\{\underline{x} \diamond \underline{y}, \underline{x} \diamond \overline{y}, \overline{x} \diamond \underline{y}, \overline{x} \diamond \overline{y}\}\,, \\ \text{and } \overline{z} &= \max\{\underline{x} \diamond \underline{y}, \underline{x} \diamond \overline{y}, \overline{x} \diamond \underline{y}, \overline{x} \diamond \overline{y}\}\,. \end{aligned} \quad (1)$$

Functions like $e^{[\underline{x}, \overline{x}]}$ and $[\underline{x}, \overline{x}]^n$ can be defined in an analogous manner. The intervalization of any monotonic or piecewise monotonic elementary function is computed by evaluating the function on a finite set of *special points*, consisting of the interval's endpoints and local extrema.

For bounding the range of a more complex expression we have to assign a corresponding *interval extension* to it. An interval-valued function $[f]$ is called an interval extension of the real-valued function f, if

$$[f]([\underline{x}_1, \overline{x}_1], \ldots, [\underline{x}_n, \overline{x}_n]) \supseteq \{f(y_1, \ldots, y_n) \,|\, y_i \in [\underline{x}_i, \overline{x}_i]\}\ . \quad (2)$$

The interval extension obtained by replacing real operations and elementary functions by their interval-valued equivalents is called *natural interval extension* [2].

2.2 The Dependence Problem and Symbolic Solutions

The major drawback in using interval computations is caused by the *dependence problem*. While computations using independent parameters will return tight bounds to the exact range of the function, two or more occurrences of the same parameter during the evaluation phase will result in too conservative estimations. For instance, consider the voltage divider circuit in Figure 1. Its behaviour can be

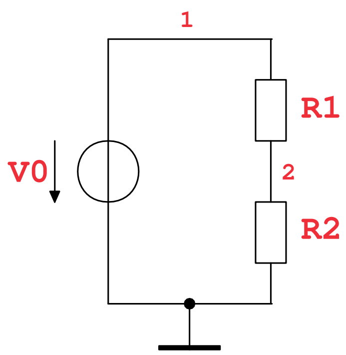

Voltage divider circuit.

Figure 1

described by the matrix equation

$$\begin{pmatrix} \frac{1}{R_1} & -\frac{1}{R_1} & 1 \\ -\frac{1}{R_1} & \frac{1}{R_1}+\frac{1}{R_2} & 0 \\ 1 & 0 & 0 \end{pmatrix} \cdot \begin{pmatrix} V_1 \\ V_2 \\ I_{V_0} \end{pmatrix} = \begin{pmatrix} 0 \\ 0 \\ V_0 \end{pmatrix} . \tag{3}$$

In this case, one can explicitely find a symbolic solution i. e. for each variable we obtain an expression in terms of V_0, R_1, and R_2

$$V_1 = V_0 \, , V_2 = \frac{R_2 \cdot V_0}{R_1 + R_2} \, , \text{and } I_{V_0} = -\frac{V_0}{R_1 + R_2} \, .$$

Assuming $V_0 = 1\,\mathrm{V}$, as well as uncertain $R_1/1\,\Omega \in [9, 11]$, and $R_2/1\,\Omega \in [90, 110]$, interval arithmetic can be used to compute rough bounds to the range with respect to these settings,

$$V_1 = 1\,\mathrm{V} \, , V_2/1\,\mathrm{V} \in [0.743, 1.112] \, , \text{and } I_{V_0}/1\,\mathrm{mA} \in [-10.1, -8.27] \, .$$

But here the voltage V_2 can be bounded more accurately. Using the equivalent reformulation $V_2 = \frac{V_0}{1+R_1/R_2}$ to compute the interval results, the essentially tighter range $V_2/1\,\mathrm{V} \in [0.891, 0.925]$ is obtained. Since each uncertain parameter occurs only once, this is the best possible result. Therefore, simply replacing numerical solvers by an interval version would soon lead to rather useless results, consisting of large parts of the original search region, which had been obtained before. Hence, no further information would be generated in this case.

Several algorithms have been developed to solve linear and nonlinear interval-valued equation systems [2, 3]. These behave well if we are dealing with intervals of small width and little dependence of the interval-valued terms of the expressions involved, but real-life applications will require the treatment of wider intervals and parameters of multiple occurrences. For our purpose interval algorithms have to be tuned for solving equation systems resulting from industrial analog circuits.

3 Fill-in Patterns of Linear Circuits

In the case of linear analog circuits with uncertain parameters Kirchhoff's laws and element relations are summarized in a matrix equation of the following form:

$$\mathbf{A}(\mathbf{p}) \cdot \mathbf{x} = \mathbf{b}\,, \tag{4}$$

where $\mathbf{x}$ denotes the vector of internal currents and voltages, and the parameter vector $\mathbf{p} = (p_1, \ldots, p_{n_p})$ corresponds to tolerance-affected components, which are bounded by intervals $[p_i]$. Solving such an interval equation system means determining close bounds to the smallest box $[\mathbf{x}]$ with

$$[\mathbf{x}] \supseteq \left\{ (\mathbf{A}(\mathbf{p}))^{-1} \cdot \mathbf{b} \,\middle|\, p_i \in [p_i] \right\} . \tag{5}$$

Note that uncertain values of independent current and voltage sources can also be modeled as interval-valued parameters on the right-hand side $\mathbf{b}$. These kind of parameters can be moved to the matrix by the cost of introducing new rows and columns.

In order to apply interval arithmetic in linear circuit analysis, it is necessary to use a real formulation of the matrix equation. Hence, a complex-valued equation system used for AC analysis needs to be reformulated [4]. The result corresponding to each variable will be wrapped by a polygon in the complex plane (*wrapping effect*).

Earlier efforts to solve interval-valued linear circuit equations were restricted to formulations, in which each matrix element varies independently [4]. Therefore a new approach was developed to cope with multiple occurrences of parameters: First of all we will assume that the parameter dependence of $\mathbf{A}(\mathbf{p})$ can be written as a sequence of rank-one updates of a parameter-independent real-valued matrix $\mathbf{A}_0 \in \mathbb{R}^{n \times n}$:

$$\mathbf{A}(\mathbf{p}) = \mathbf{A}_0 + \sum_{i=1}^{n_\mathbf{p}} p_i \cdot (\mathbf{u}_i \cdot \mathbf{v}_i^\mathsf{T})\,, \tag{6}$$

with $\mathbf{u}_i, \mathbf{v}_i \in \mathbb{R}^n$, and $\mathbf{A}(\mathbf{p})$ is invertible for all $\mathbf{p} \in [\mathbf{p}]$. This is not a restriction at all, because this structure is already inherent to a linear circuit: Using the *sparse tableau formulation* (*STA*) [5] to generate the linear circuit equations, each p_i will occur only once and $\mathbf{u}_i, \mathbf{v}_i$ are just unit vectors, which define the corresponding matrix element. In the case of *modified nodal analysis* (*MNA*) [5] the matrices of the form $p_i \cdot (\mathbf{u}_i \cdot \mathbf{v}_i^\top)$ correspond to the well-known fill-in patterns used during equation setup.

4 Mathematical Methods

In this section we restrict ourselves to the treatment of linear circuit elements. Earlier efforts to solve interval-valued linear circuit equations were restricted to formulations, in which each matrix element varies independently [4]. Therefore a new approach was developed to cope with multiple occurrences of parameters: we have already seen in Section 3 that a resistive circuit may be represented by the parametric matrix equation $\mathbf{A}(\mathbf{p}) \cdot \mathbf{x} = \mathbf{b}$, whose parameter dependence can be written in the fill-in pattern form of Equation 5. It has already been pointed out independently by Dreyer [6] and Ganesan et al. [7], that the rank-one updates forming these systems emit useful monotonicity properties.

In case that capacitances and inductanctes are involved, the structure is likewise, but the corresponding p_i may vary on the imaginary axis instead. In any case, it can be utilized for efficient solving of interval-valued circuit equations [8].

4.1 Methods for Resistive Circuits

The *Sherman-Morrison formula* [9] allows for inverting a perturbed matrix for a change to a given matrix without inverting the whole matrix again.

Theorem 4.1 (Sherman-Morrison) *Let $\mathbf{A} \in \mathbb{R}^{n\times n}$ be invertible and $\mathbf{u}, \mathbf{v} \in \mathbb{R}^n$. Then the matrix $\mathbf{A} + \mathbf{u} \cdot \mathbf{v}^\top$ is invertible if and only if $1 + \mathbf{v}^\top \mathbf{A}^{-1}\mathbf{u} \neq 0$. In this case we have:*

$$(\mathbf{A} + \mathbf{u} \cdot \mathbf{v}^\top)^{-1} = \mathbf{A}^{-1} - \frac{1}{1 + \mathbf{v}^\top \mathbf{A}^{-1}\mathbf{u}} \mathbf{A}^{-1}\mathbf{u}\mathbf{v}^\top \mathbf{A}^{-1} \,. \tag{7}$$

The relationship between determinants of original and changed matrix is exploited in the following.

Corollary 4.2 *Let* $\mathbf{A} \in \mathbb{R}^{n\times n}$ *and* $\mathbf{u}, \mathbf{v} \in \mathbb{R}^n$*. Then*

$$\det(\mathbf{A} + \mathbf{u} \cdot \mathbf{v}^\intercal) = \det(\mathbf{A}) \cdot \det(1 + \mathbf{v}^\intercal \mathbf{A}^{-1}\mathbf{u})\,.$$

There is also a slightly more general version of the theorem.

Theorem 4.3 (Sherman-Morrison-Woodbury) *Let* $\mathbf{A} \in \mathbb{R}^{n\times n}$ *be an invertible matrix, and let* $\mathbf{U}, \mathbf{V} \in \mathbb{R}^{m\times n}$ *with* $m \leq n$*. Then* $\mathbf{A} + \mathbf{U} \cdot \mathbf{V}^\intercal$ *is invertible if and only if* $1 + \mathbf{V}^\intercal \mathbf{A}^{-1}\mathbf{U}$ *is invertible. In this case we have:*

$$(\mathbf{A} + \mathbf{U} \cdot \mathbf{V}^\intercal)^{-1} = \mathbf{A}^{-1} - \mathbf{A}^{-1}\mathbf{U}\left(1 + \mathbf{V}^\intercal \mathbf{A}^{-1}\mathbf{U}\right)^{-1} \mathbf{V}^\intercal \mathbf{A}^{-1}\,.$$

For a detailed proof of the theorems see [9] or [11]. The latter also incorporates a proof of the corollary.

Equation 7 has already been used in the field of analog circuit analysis for calculating the influence of a single matrix entry to the solution [12, 13]. Linear equations in fill-in pattern form perfectly fit into the conditions of the Sherman-Morrison formula.

In order to show some properties of the fill-in pattern form Theorem 4.1 can be applied.

Theorem 4.4 (Convex-hull theorem for fill-in patterns)
Let $[\mathbf{p}] \in [\mathbb{R}]^{n_\mathbf{p}}$*, and let* $\mathbf{A}(\mathbf{p}) = \mathbf{A}_0 + \sum_{i=1}^{n_\mathbf{p}} p_i \cdot (\mathbf{u}_i \cdot \mathbf{v}_i^\intercal)$ *with* $\mathbf{u}_i, \mathbf{v}_i \in \mathbb{R}^n$ *be invertible for all* $\mathbf{p} \in [\mathbf{p}]$*.*

Then $\mathbf{A}(\mathbf{p})^{-1} \cdot \mathbf{b}$ *is (componentwise) monotonic and continuous in* p_i *for all* $i = 1, \ldots, n_\mathbf{p}$*. Furthermore, the following holds*

$$\operatorname{conv}\left\{\mathbf{A}(\mathbf{p})^{-1} \cdot \mathbf{b} \,\middle|\, \mathbf{p} \in [\mathbf{p}]\right\} = \operatorname{conv}\left\{\mathbf{A}(\mathbf{p})^{-1} \cdot \mathbf{b} \,\middle|\, \mathbf{p} \in \operatorname{corners}([\mathbf{p}])\right\}\,.$$

Proof: Since all parameters $p_1, \ldots, p_{n_\mathbf{p}}$ may vary independently, it sufficies to show the theorem for $n_\mathbf{p} = 1$. We may also assume, that $\mathbf{A}_0$ is invertible, because $\mathbf{A}_0$ can be replaced by $\mathbf{A}(\mathbf{p}_0)$ if exchanging $\mathbf{p}$ by $\mathbf{p} - \mathbf{p}_0$ for a fixed parameter setting $\mathbf{p}_0 \in [\mathbf{p}]$.

Then application of *Sherman-Morrison* leads to

$$(\mathbf{A}_0 + p \cdot (\mathbf{u}\,\mathbf{v}^\intercal))^{-1}\,\mathbf{b} = \mathbf{A}_0^{-1}\,\mathbf{b} - \frac{p}{1 + p \cdot \mathbf{v}^\intercal \mathbf{A}_0^{-1}\mathbf{u}} \mathbf{A}_0^{-1}\mathbf{u}\mathbf{v}^\intercal \mathbf{A}_0^{-1}\,\mathbf{b}\,,$$

whose continuity follows directly from the Theorem 4.1. The monotonic property with respect to p can easily be derived using elementary calculations on the right-hand side.

Finally, the last part of the theorem is a consequence of Farkas's Lemma [14]. Following, we will denote $\mathbf{x_p} := \mathbf{A}(\mathbf{p})^{-1} \cdot \mathbf{b}$ for all $\mathbf{p} \in \mathrm{corners}\,([\mathbf{p}])$. We shall prove that the system of linear equations

$$\sum_{\mathbf{p} \in \mathrm{corners}([\mathbf{p}])} \lambda_\mathbf{p} \, \mathbf{x_p} \quad = \quad \mathbf{x}_0 \tag{8}$$

$$\sum_{\mathbf{p} \in \mathrm{corners}([\mathbf{p}])} \lambda_\mathbf{p} \quad = \quad 1 \tag{9}$$

has a non-negative solution $(\lambda_\mathbf{p})_{\mathbf{p} \in \mathrm{corners}([\mathbf{p}])}$. By Farkas's Lemma it is sufficient to show that for each $\mathbf{q} \in \mathbb{R}^n$, $q_0 \in \mathbb{R}$, if $\mathbf{q}^\mathsf{T} \cdot \mathbf{x_p} + q_0 \geq 0,$ for all $\mathbf{p} \in \mathrm{corners}\,([\mathbf{p}])$. Then we have

$$\mathbf{q}^\mathsf{T} \cdot \mathbf{x}_0 + q_0 \geq 0\,.$$

Assume now, that $\mathbf{q}$ and q_0 are chosen such that

$$\mathbf{q}^\mathsf{T} \cdot \mathbf{x_p} + q_0 \geq 0, \text{ for all } \mathbf{p} \in \mathrm{corners}\,([\mathbf{p}])\ .$$

Since the monotonicity argument also holds for $f(\mathbf{p}) := \mathbf{q}^\mathsf{T} \cdot \mathbf{x_p}$, there exists a vector $\mathbf{p} \in \mathrm{corners}\,([\mathbf{p}])$ with $\mathbf{q}^\mathsf{T} \cdot \mathbf{x_p} \leq \mathbf{q}^\mathsf{T} \cdot \mathbf{x}_0$, and hence,

$$\mathbf{q}^\mathsf{T} \cdot \mathbf{x}_0 + q_0 \geq \mathbf{q}^\mathsf{T} \cdot \mathbf{x_p} + q_0 \geq 0$$

yields the desired relation. □

If regularity of $\mathbf{A}(\mathbf{p})$ can be established for all $\mathbf{p} \in [\mathbf{p}]$, Theorem 4.4 can be used to compute sharp bounds to the solution set of an uncertain linear system in fill-in pattern form. The following lemma yields an equivalent condition to the regularity of $\mathbf{A}(\mathbf{p})$, which can be computed efficiently.

Lemma 4.5 (Regularity test) *Let*

$$\mathbf{A}(\mathbf{p}) = \mathbf{A}_0 + \sum_{i=1}^{n_\mathbf{p}} p_i \cdot (\mathbf{u}_i \cdot \mathbf{v}_i^\mathsf{T})$$

with $\mathbf{u}_i, \mathbf{v}_i \in \mathbb{R}^n$. Then $\mathbf{A}(\mathbf{p})$ is invertible for all $\mathbf{p} \in [\mathbf{p}]$ if and only if the value $\mathrm{sign}\det(\mathbf{A}(\mathbf{p}))$ is non-zero and constant for all $\mathbf{p} \in \mathrm{corners}\,([\mathbf{p}])$.

Proof: One only has to show, that a sign change in $\det(\mathbf{A}(\mathbf{p}))$ immediately yields a parameter setting $\mathbf{p}_0 \in [\mathbf{p}]$, such that $\mathbf{A}(\mathbf{p}_0)$ is singular. Therefore, suppose there were some corner points $\mathbf{p}_\nu$ and $\mathbf{p}_\mu$ such that the inequality $\det \mathbf{A}(\mathbf{p}_\nu) < 0 < \det \mathbf{A}(\mathbf{p}_\mu)$ holds. Without loss of generality both points only differ in one parameter component p_i. By Corollary 4.2 we know that $\det \mathbf{A}(\mathbf{p})$ is of the form

$$\det \mathbf{A}(\mathbf{p}) = f(p_i) := a + p_i \cdot b\,, \tag{10}$$

for real values a and b not depending on p_i. But a sign change of this function means that there exists a p_i^* in range with $f(p_i^*) = 0$, which is a contradiction to the fact, that the determinant must not be zero. □

The regularity test can now be used in combination with Theorem 4.4 for computing sharp bounds to the range of $\mathbf{A}(\mathbf{p})^{-1} \cdot \mathbf{b}$ over $[\mathbf{p}]$, for $\mathbf{A}(\mathbf{p})$ in fill-in pattern form. This results in $2^{n_\mathbf{p}}$ linear systems to be processed. An interval hull can easily be obtained from a convex set by componentwise calculating minimum and maximum values. The whole procedure is exposed in Algorithm 1.

Algorithm 1 Real-valued linear system solver

Input: $\mathbf{A}(\mathbf{p}) \in \mathbb{R}^{n \times n}$ in the form of Theorem 4.4, $\mathbf{b} \in \mathbb{R}^n$, and $[\mathbf{p}] \in [\mathbb{R}]^{n_\mathbf{p}}$
Output: $S = \{\mathbf{x}_1, \ldots, \mathbf{x}_{2^{n_\mathbf{p}}}\}$ such that $\mathbf{A}(\mathbf{p})^{-1}\, \mathbf{b} \in \operatorname{conv}(S)$, for all $\mathbf{p} \in [\mathbf{p}]$

```
Set s := sign(det A(p_0)) for some p_0 ∈ [p].
if s = 0 then
  return failed
end if
Set S := ∅.
for p ∈ corners([p]) do
  /* Regularity test */
  if det A(p) ≠ s then
    return failed
  else
    S := S ∪ {A(p)^{-1} · b}
  end if
end for
```

The advantage of Algorithm 1 is, that it does not need interval computations. Of course, interval arithmetic can be used to bound rounding errors. In the case that these do not have to be tracked, already existing numerical solvers, like those of analog circuit simulators [15, 16], can be utilized for tolerance analysis.

Example As example, we reconsider the voltage divider circuit of Figure 1, whose circuit equations can be written as the following matrix equations

$$\begin{pmatrix} \frac{1}{R_1} & -\frac{1}{R_1} & 1 \\ -\frac{1}{R_1} & \frac{1}{R_1} + \frac{1}{R_2} & 0 \\ 1 & 0 & 0 \end{pmatrix} \cdot \begin{pmatrix} V_1 \\ V_2 \\ I_{V_0} \end{pmatrix} = \begin{pmatrix} 0 \\ 0 \\ V_0 \end{pmatrix}, \qquad (11)$$

for fixed $V_0 = 1\,\mathrm{V}$ and uncertain $R_1/1\,\Omega \in [9, 11]$, and $R_2/1\,\Omega \in [90, 110]$.

Since there is a one-to-one correspondence between the endpoints of R_i and $1/R_i$, one can immediately apply Algorithm 1 to the system.

Hence, it is enough to solve these equations for the four corner points

$$\text{corners}\begin{pmatrix}[9,11]\\ [90,110]\end{pmatrix} = \left\{\begin{pmatrix}9\\90\end{pmatrix},\begin{pmatrix}9\\110\end{pmatrix},\begin{pmatrix}11\\90\end{pmatrix},\begin{pmatrix}11\\110\end{pmatrix}\right\},$$

which results approximately in the convex solution set

$$\begin{pmatrix}V_1\\V_2\\I_{V_0}\end{pmatrix} \in \text{conv}\left\{\begin{pmatrix}1\\0.909\\-0.0101\end{pmatrix},\begin{pmatrix}1\\0.925\\-0.0084\end{pmatrix},\begin{pmatrix}1\\0.891\\-0.0099\end{pmatrix},\begin{pmatrix}1\\0.909\\-0.00827\end{pmatrix}\right\},$$

i. e. for the given tolerances we have $V_1 = 1\,\mathrm{V}$, and the remaining voltage and current are bounded as $V_2/1\,\mathrm{V} \in [0.891, 0.925]$, and $I_{V_0}/1\,\mathrm{mA} \in [-10.1, -8.27]$.

4.2 A faster approach

The approach described above is suitable for small parameter numbers $n_{\mathbf{p}}$ only, because the interval-valued problem is put down to the solution of $2^{n_{\mathbf{p}}}$ real-valued linear systems. In order to treat a large number of parameters, we use a kind of intervalization of the Sherman-Morrison formula to obtain a less accurate, but faster algorithm. As seen in the case of a single uncertain parameter $p \in [\underline{p}, \overline{p}]$, the solution is given as

$$\mathbf{A}(p)^{-1}\mathbf{b} = \mathbf{A}(p_0)^{-1}\,\mathbf{b} - \frac{p-p_0}{d(p)}\mathbf{A}(p_0)^{-1}\mathbf{u}\,\mathbf{v}^\mathsf{T}\mathbf{A}(p_0)^{-1}\,\mathbf{b}\,, \tag{12}$$

if we set $d(p) = 1 + (p - p_0)\cdot \mathbf{v}^\mathsf{T}\mathbf{A}(p_0)^{-1}\mathbf{u}$ for a fixed value $p_0 \in [\underline{p}, \overline{p}]$ under the conditions of the Sherman-Morrison theorem. But the latter can also be applied, in case one is able to show that $d(p) \neq 0$ for all $p \in [\underline{p}, \overline{p}]$. This can efficiently be calculated by evaluating

$$d([\underline{p}, \overline{p}]) = 1 + ([\underline{p}, \overline{p}] - p_0)\cdot(\mathbf{v}^\mathsf{T}\mathbf{A}(p_0)^{-1}\mathbf{u}) \tag{13}$$

using interval arithmetic. Hence, it can be verified, whether $d([\underline{p}, \overline{p}]) \not\ni 0$. If that is the case, the range of the factor $[\underline{m}, \overline{m}] := (p - p_0)/d(p)$ over all $p \in [\underline{p}, \overline{p}]$ is exactly bounded by

$$\underline{m} = ((\underline{p} - p_0)^{-1} + \mathbf{v}^\mathsf{T}\mathbf{A}_0^{-1}\mathbf{u})^{-1} \quad \text{and} \quad \overline{m} = ((\overline{p} - p_0)^{-1} + \mathbf{v}^\mathsf{T}\mathbf{A}_0^{-1}\mathbf{u})^{-1}. \tag{14}$$

At this point all essential parts for bounding Equation 13 are available. Indeed, this forms an interval-valued version of the Sherman-Morrison formula.

Theorem 4.6 (Interval-valued Sherman-Morrison) *Let $\mathbf{A} \in \mathbb{R}^{n\times n}$ be invertible and $\mathbf{u}, \mathbf{v} \in \mathbb{R}^n$. Then the matrix $\mathbf{A} + p\cdot\mathbf{u}\,\mathbf{v}^\mathsf{T}$ is invertible for all $p \in [\underline{p}, \overline{p}]$ if and only if*

$$1 + ([p] - p_0)\cdot(\mathbf{v}^\mathsf{T}\mathbf{A}(p_0)^{-1}\mathbf{u}) \not\ni 0 \tag{15}$$

In this case, we can calculate for a right-hand side $\mathbf{b} \in \mathbb{R}^n$*:*

$$\left(\mathbf{A} + [\underline{p}, \overline{p}] \cdot \mathbf{u}\,\mathbf{v}^\intercal\right)^{-1} \mathbf{b} = \mathbf{A}^{-1}\mathbf{b} - [\underline{m}, \overline{m}] \cdot \left(\mathbf{A}^{-1}\mathbf{u}\mathbf{v}^\intercal\mathbf{A}^{-1}\mathbf{b}\right) \tag{16}$$

with $[\underline{m}, \overline{m}] = [((\underline{p} - p_0)^{-1} + \mathbf{v}^\intercal\mathbf{A}_0^{-1}\mathbf{u})^{-1}, ((\overline{p} - p_0)^{-1} + \mathbf{v}^\intercal\mathbf{A}_0^{-1}\mathbf{u})^{-1}]$.

Proof: Due to the calculations above and the Sherman-Morrison formula, it only remains to motivate the computation of $\underline{m}$ and $\overline{m}$. The range of $[\underline{m}, \overline{m}]$ results from the valuable property of interval arithmetic, that certain kinds of divisions by zero are allowed. This includes $1/[0, b] = [1/b, \infty]$, and $1/[a, 0] = [-\infty, 1/a]$, which can be used to describe the range of

$$1/[a, b] = [-\infty, 1/a] \cup [1/b, \infty]\,, \text{ for } a < 0 < b\,. \tag{17}$$

Hence, for $p_0 \in [\overline{p}, \underline{p}]$ one can compute the range of $d(p) := 1/(p - p_0) + \mathbf{v}^\intercal\mathbf{A}_0^{-1}\mathbf{u}$ over $p \in [\underline{p}, \overline{p}]$ as

$$\begin{aligned} d([\overline{p}, \underline{p}]) &= 1/[\overline{p} - p_0, \underline{p} - p_0] + \mathbf{v}^\intercal\mathbf{A}_0^{-1}\mathbf{u} \\ &= [-\infty, (\underline{p} - p_0)^{-1} + \mathbf{v}^\intercal\mathbf{A}_0^{-1}\mathbf{u})] \cup [(\overline{p} - p_0)^{-1} + \mathbf{v}^\intercal\mathbf{A}_0^{-1}\mathbf{u}, \infty]\,. \end{aligned}$$

If Equation 15 holds, then both intervals obtained by these calculations do not include zero. Then inverting and reunifying the resulting intervals yields the regular interval $1/d([\overline{p}, \underline{p}]) = [\underline{m}, \overline{m}]$. □

For illustration, the voltage divider example of Section 4.1 is treated again, with fixed $R_2 = 100\,\Omega$ and $V_0 = 1\,\mathrm{V}$. Hence, we have

$$\begin{pmatrix} \frac{1}{R_1} & -\frac{1}{R_1} & 1 \\ -\frac{1}{R_1} & \frac{1}{R_1} + 0.01 & 0 \\ 1 & 0 & 0 \end{pmatrix} \cdot \begin{pmatrix} V_1 \\ V_2 \\ I_{V_0} \end{pmatrix} = \begin{pmatrix} 0 \\ 0 \\ 1 \end{pmatrix}, \tag{18}$$

interpreting $\frac{1}{R_1}$ as parameter with $p \equiv \frac{1}{R_1} \in [\underline{p}, \overline{p}] = 1/[9, 11] = [0.0909, 0.1112]$, the fill-in pattern and the matrix $\mathbf{A}_0$ with respect to $p_0 = 0.1$ are given by

$$\mathbf{u} = \begin{pmatrix} 1 \\ -1 \\ 0 \end{pmatrix}, \mathbf{v} = \begin{pmatrix} 1 \\ -1 \\ 0 \end{pmatrix}, \text{ and } \mathbf{A}_0 = \begin{pmatrix} 0.1 & -0.1 & 1 \\ -0.1 & 0.11 & 0 \\ 1 & 0 & 0 \end{pmatrix}$$

One immediately computes

$$\mathbf{A}_0^{-1}\mathbf{b} = \begin{pmatrix} 1 \\ 0.909 \\ -0.009 \end{pmatrix} \text{ and } \mathbf{A}_0^{-1}\mathbf{u} = \begin{pmatrix} 1 \\ -9.0909 \\ 0.0909 \end{pmatrix}.$$

Because $\mathbf{v}^\mathsf{T}\mathbf{A}_0^{-1}\mathbf{u} = 9.0909$, $\frac{1}{\underline{p}-p_0} = -110$, and $\frac{1}{\overline{p}-p_0} = 90$, the system is invertible for all p. Hence, the factor

$$[x] = [1/(-110 + 9.0909), 1/(90 + 9.0909)] = [-0.0099, 0.0101]$$

may be calculated. Using Equation 16 we get tight bounds to the solution: $V_1 = 1\,\mathrm{V}$, as well as $V_2/1\,\mathrm{V} \in [0.900, 0.918]$ and $I_{V_0}/1\,\mathrm{mA} \in [-9.2, -9]$.

Reintroducing the second uncertain parameter $\frac{1}{R_2}$ from the example, one can clearly set $q \equiv \frac{1}{R_2} \in [q] = [0.009, 0.012]$, $q_0 = 0.01$ with fill-in patterns corresponding to the vectors

$$\mathbf{y} = \begin{pmatrix} 0 \\ 1 \\ 0 \end{pmatrix} \text{ and } \mathbf{z} = \begin{pmatrix} 0 \\ 1 \\ 0 \end{pmatrix}.$$

For tracking the variations of $\left(\mathbf{A}_0 + p \cdot \mathbf{u}\mathbf{v}^\mathsf{T} + q \cdot \mathbf{y}\mathbf{z}^\mathsf{T}\right)^{-1}\mathbf{b}$ due to both p and q the interval-valued Sherman-Morrison formula may be applied a second time. But for this purpose one cannot continue to use a real-valued matrix $\mathbf{A}_0$, instead it has to replaced by all possible matrices $\mathbf{A}(p) = \mathbf{A}_0 + p \cdot \mathbf{u}\mathbf{v}^\mathsf{T}$ in range. The necessary intermediate results $\mathbf{A}(p)^{-1}\mathbf{b}$ and $\mathbf{A}(p)^{-1}\mathbf{y}$ can be bounded for $p \in [p]$ by interval-vectors with the method described above. In particular,

$$\mathbf{A}([p])^{-1}\mathbf{y} = \begin{pmatrix} 0 \\ [8.181, 10] \\ [0.891, 0.9244] \end{pmatrix} \text{ and } \mathbf{A}([p])^{-1}\mathbf{b} = \begin{pmatrix} 1 \\ [0.900, 0.918] \\ [-0.0092, -0.009] \end{pmatrix},$$

whereas the latter was already computed above. Analogously, we obtain

$$-\mathbf{z}^\mathsf{T}\mathbf{A}([p])^{-1}\mathbf{y} = [-10, -8.181]\,,$$

which indeed lies between $\frac{1}{\underline{q}-q_0} = -1100$, and $\frac{1}{\overline{q}-q_0} = 900$. Therefore, we can go on to calculate the factor $[x_2] = [-0.00092, 0.0012]$, and finally the value $\mathbf{z}^\mathsf{T}\mathbf{A}([p])^{-1}\mathbf{b} = [0.900, 0.918]$ is obtained.

The final solution can be computed by evaluating

$$\mathbf{A}([p])^{-1}\mathbf{b} - [x_2] \cdot \left(\mathbf{A}([p])^{-1}\mathbf{y}\right) \cdot \left(\mathbf{z}^\mathsf{T}\mathbf{A}([p])^{-1}\mathbf{b}\right) =$$
$$\begin{pmatrix} 1 \\ [0.900, 0.918] \\ [-0.0092, -0.009] \end{pmatrix} - [-0.0009, 0.0012] \cdot \begin{pmatrix} 0 \\ [8.181, 10] \\ [0.891, 0.9244] \end{pmatrix} \cdot [0.9, 0.918]\,,$$

which leads to $V_1 = 1\,\mathrm{V}$, and

$$V_2/1\,\mathrm{V} \in [0.8908, 0.926]\,, \text{ and } I_{V_0}/1\,\mathrm{A} \in [-0.0102, -0.00824]\,.$$

This result contains slightly larger intervals than the one obtained in Section 4.1. The reason for this is, that the parameter interval $[p]$ occurs more than once during the evaluation procedure, because $\mathbf{A}([p])^{-1}\mathbf{b}$ as well as $\mathbf{A}([p])^{-1}\mathbf{y}$ depend on it.

The advantage of this approach is that it can easily be extented to $n_{\mathbf{p}}$ parameters $p_\nu \in [\underline{p}_\nu, \overline{p}_\nu]$ and corresponding fill-in patterns $\mathbf{u}_\nu \, \mathbf{v}_\nu^{\mathsf{T}}$ for $\nu = 1, \ldots, n_{\mathbf{p}}$. After fixing a vector $\mathbf{p}_0 = \left(p_{1,0}, \ldots, p_{n_{\mathbf{p}},0}\right)^{\mathsf{T}}$, with $p_{\nu,0} \in [\underline{p}_\nu, \overline{p}_\nu]$, the procedure is initialized by simultaneously computing

$$[\tilde{\mathbf{b}}] := \mathbf{A}(\mathbf{p}_0)^{-1} \cdot \mathbf{b} \text{ and } [\tilde{\mathbf{u}}_\nu] := \mathbf{A}(\mathbf{p}_0)^{-1} \cdot \mathbf{u}_\nu \text{ for all } \nu \,.$$

If in the i^{th} step the condition $(\underline{p}_i - p_{i,0})^{-1} < -\mathbf{v}_i^{\mathsf{T}} \cdot [\tilde{\mathbf{u}}_i] < (\overline{p}_i - p_{i,0})^{-1}$ holds, i interval vectors have to be updated in the following scheme

$$\begin{aligned}
[x] &\leftarrow [\Big((\underline{p}_i - p_{i,0})^{-1} + \max \mathbf{v}_i^{\mathsf{T}} \cdot [\tilde{\mathbf{u}}_i]\Big)^{-1}, \Big((\overline{p}_i - p_{i,0})^{-1} + \min \mathbf{v}_i^{\mathsf{T}} \cdot [\tilde{\mathbf{u}}_i]\Big)^{-1}] \\
[\tilde{\mathbf{b}}] &\leftarrow [\tilde{\mathbf{b}}] - [x] \cdot [\tilde{\mathbf{u}}_i] \cdot \Big(\mathbf{v}_i^{\mathsf{T}} \cdot [\tilde{\mathbf{b}}]\Big) \qquad (19) \\
[\tilde{\mathbf{u}}_j] &\leftarrow [\tilde{\mathbf{u}}_j] - [x] \cdot [\tilde{\mathbf{u}}_i] \cdot \Big(\mathbf{v}_i^{\mathsf{T}} \cdot [\tilde{\mathbf{u}}_j]\Big) \,, \text{ for } j > i \,.
\end{aligned}$$

The brackets in the last term of each line force computation of the vector products ${\mathbf{v}_i}^{\mathsf{T}} \cdot [\tilde{\mathbf{b}}]$ and ${\mathbf{v}_i}^{\mathsf{T}} \cdot [\tilde{\mathbf{u}}_j]$ prior to the multiplication with $[\tilde{\mathbf{u}}_i]$.

This is more efficient than the algebraic equivalent sequences

$$([\tilde{\mathbf{u}}_j] \cdot {\mathbf{v}_i}^{\mathsf{T}}) \cdot [\tilde{\mathbf{b}}] \text{ and } ([\tilde{\mathbf{u}}_j] \cdot {\mathbf{v}_i}^{\mathsf{T}}) \cdot [\tilde{\mathbf{u}}_j] \,,$$

respectively, which generate interval-valued matrices first. The latter would cause additional pessimism due to the dependence problem.

The procedure is summarized in Algorithm 2. The number of evaluations of formula 16 is of order $\mathcal{O}(n_{\mathbf{p}}^2)$. Hence, this approach is much more suited to the treatment of a large number of uncertain parameters than Algorithm 1. But the lower complexity is payed back by reduced accuracy, because interdependences are not removed completely.

Algorithm 2 Quick real-valued linear system solver

Input: $\mathbf{A}(\mathbf{p}) = \mathbf{A}_0 + \sum_{i=1}^{n_\mathbf{p}} p_i \cdot (\mathbf{u}_i\, \mathbf{v}_i^\mathsf{T}) \in \mathbb{R}^{n\times n}$ in the form of Theorem 4.4, $\mathbf{b} \in \mathbb{R}^n$, and $\mathbf{p} \in [\mathbf{p}] \in [\mathbb{R}]^{n_\mathbf{p}}$

Output: $[\mathbf{x}] \supseteq \mathbf{\Sigma}(\mathbf{A}(\mathbf{p}), \mathbf{b})$, for all $\mathbf{p} \in [\mathbf{p}]$

Select $\mathbf{p}_0 \in [\mathbf{p}]$, set $[\tilde{\mathbf{p}}] := [\mathbf{p}] - \mathbf{p}_0$.
for $i := 1, \ldots, n_\mathbf{p}$ **do**
  Set $[\tilde{\mathbf{u}}_i] := \mathbf{A}_0^{-1} \cdot \mathbf{u}_i$.
end for
Set $[\tilde{\mathbf{u}}_{n_\mathbf{p}+1}] := \mathbf{A}_0^{-1} \cdot \mathbf{b}$, $S := \{[\tilde{\mathbf{u}}_i] \,|\, i = 1, \ldots, n_\mathbf{p} + 1\}$.
for $i = 1, \ldots, n_\mathbf{p}$ **do**
  Set $S := S \setminus \{[\tilde{\mathbf{u}}_i]\}$
  /* Regularity test */
  if $1/\min[\tilde{p}_i] < -\mathbf{v}_i^\mathsf{T} \cdot [\tilde{\mathbf{u}}_i] < 1/\max[\tilde{p}_i]$ **then**
    $[x] = [(1/\min[\tilde{p}_i] + \max \mathbf{v}_i^\mathsf{T} \cdot [\tilde{\mathbf{u}}_i])^{-1}, (1/\max[\tilde{p}_i] + \min \mathbf{v}_i^\mathsf{T} \cdot [\tilde{\mathbf{u}}_i])^{-1}]$
    for $[\tilde{\mathbf{u}}] \in S$ **do**
      $[\tilde{\mathbf{u}}] := [\tilde{\mathbf{u}}] - [x] \cdot [\tilde{\mathbf{u}}_i] \cdot (\mathbf{v}_i^\mathsf{T} \cdot [\tilde{\mathbf{u}}])$
    end for
  else
    return failed
  end if
end for
$[\mathbf{x}] := [\tilde{\mathbf{u}}_{n_\mathbf{p}+1}]$

5 Frequency-Response Analysis

The small-signal analysis of analog circuits can be achieved by solving complex-valued linear systems, which are also in fill-in pattern form. Therefore, we will assume, that $\mathbf{C} \in \mathbb{C}^{n\times n}$ is invertible and the parameter dependence is given by

$$\mathbf{C}(\mathbf{p}) = \mathbf{C}_0 + \sum_{\nu=1}^{n_\mathbf{p}} p_\nu \cdot e^{i\varphi_\nu} \cdot (\mathbf{u}_\nu \cdot \mathbf{v}_\nu^\mathsf{T})$$

with $\mathbf{u}_\nu, \mathbf{v}_\nu \in \mathbb{R}^n$ and uncertain parameters $p_\nu \in \mathbb{R}$ with corresponding (but certain) complex phase φ_ν. The latter is not a restriction at all, because usually the parameters in analog circuit analysis vary either on the real or on the imaginary axis.

In order to apply (real) interval techniques it is necessary to reformulate the complex-valued equation system

$$\mathbf{C} \cdot \mathbf{x} = \mathbf{d}$$

by the following equivalent real representation $\mathbf{A} \cdot \mathbf{x} = \mathbf{b}$ with

$$\mathbf{A} = \begin{pmatrix} \operatorname{Re}\mathbf{C} & -\operatorname{Im}\mathbf{C} \\ \operatorname{Im}\mathbf{C} & \operatorname{Re}\mathbf{C} \end{pmatrix}, \mathbf{x} = \begin{pmatrix} \operatorname{Re}\mathbf{x} \\ \operatorname{Im}\mathbf{x} \end{pmatrix} \text{ and } \mathbf{b} = \begin{pmatrix} \operatorname{Re}\mathbf{d} \\ \operatorname{Im}\mathbf{d} \end{pmatrix}. \quad (20)$$

This follows immediately from the complex expansion. The parameter dependence can therefore be written as

$$\mathbf{A}(\mathbf{p}) = \mathbf{A}_0 + \sum_{\nu=1}^{n_\mathbf{p}} p_\nu \cdot (\mathbf{u}_{\mathrm{up},\nu} \cdot \mathbf{v}_{\mathrm{up},\nu}{}^\mathsf{T} + \mathbf{u}_{\mathrm{low},\nu} \cdot \mathbf{v}_{\mathrm{low},\nu}{}^\mathsf{T}), \quad (21)$$

where the vectors $\mathbf{u}_{\mathrm{up},\nu} = (\mathbf{u}_\nu, 0)^\mathsf{T}$ and $\mathbf{v}_{\mathrm{up},\nu} = (\cos\varphi_\nu \cdot \mathbf{v}_\nu, -\sin\varphi_\nu \cdot \mathbf{v}_\nu)^\mathsf{T}$ denote the dependences of the upper part of the matrix $\mathbf{A}(\mathbf{p})$, while the vectors $\mathbf{u}_{\mathrm{low},\nu} = (0, \mathbf{u}_\nu)^\mathsf{T}$ and $\mathbf{v}_{\mathrm{low},\nu} = (\sin\varphi_\nu \cdot \mathbf{v}_\nu, \cos\varphi_\nu \cdot \mathbf{v}_\nu)^\mathsf{T}$ corresponds to the lower part, respectively. By introducing new parameters $p_{\mathrm{up},\nu}, p_{\mathrm{low},\nu} := p_\nu$ the parameter dependence of Equation21 can be reformulated to the form used in Section 4:

$$\mathbf{A}(\mathbf{p}) = \mathbf{A}_0 + \sum_{\nu=1}^{n_\mathbf{p}} p_{\mathrm{up},\nu} \cdot (\mathbf{u}_{\mathrm{up},\nu} \cdot \mathbf{v}_{\mathrm{up},\nu}{}^\mathsf{T}) + \sum_{\nu=1}^{n_\mathbf{p}} p_{\mathrm{low},\nu} \cdot (\mathbf{u}_{\mathrm{low},\nu} \cdot \mathbf{v}_{\mathrm{low},\nu}{}^\mathsf{T}). \quad (22)$$

Note, that this approach will suffer from the dependence problem, because the parameters $p_{\mathrm{up},\nu}$ and $p_{\mathrm{low},\nu}$ are treated independently and hence, the dependence between lower and upper part of $\mathbf{A}(\mathbf{p})$ is lost. In Figure 2 the overestimation of the range is illustrated. In order to obtain a tight wrapping of the solution set (red triangle in Figure 2).

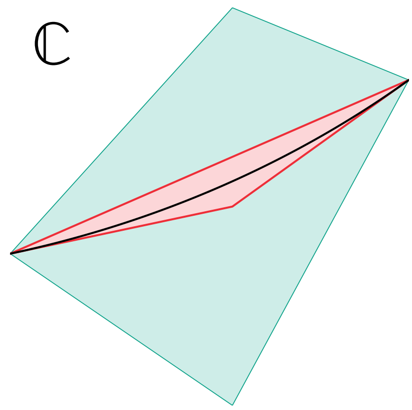

Figure 2 Single parameter variance. Real representation (quadrangle), and tight wrapping (red triangle).

The pair of vectors $\mathbf{u}_{\mathrm{low},\nu}, \mathbf{v}_{\mathrm{low},\nu}$ on the one hand, and $\mathbf{u}_{\mathrm{up},\nu}, \mathbf{v}_{\mathrm{up},\nu}$ on the other, share the valuable property, that

$$\mathbf{u}_{\mathrm{low},\nu} = \begin{pmatrix} 0 & -1 \\ 1 & 0 \end{pmatrix} \cdot \mathbf{u}_{\mathrm{up},\nu} \quad \text{and} \quad \mathbf{v}_{\mathrm{low},\nu} = \begin{pmatrix} 0 & -1 \\ 1 & 0 \end{pmatrix} \cdot \mathbf{v}_{\mathrm{up},\nu}. \quad (23)$$

In order to give explicit fomulae for the triangle's corners, we first have to show some lemmas. First, we start with a problem in $\mathbb{R}^{2\times 2}$, which can be shown using Cramer's rule.

Lemma 5.1 *Let $p_0 \in \mathbb{R}$, and let $\mathbf{A} \in \mathbb{R}^{2\times 2}$ be a matrix such that $\mathbf{A} + p \cdot 1$ be invertible for all $p \geq p_0 \in \mathbb{R}$. Furthermore, assume that*

$$\mathbf{A} = \begin{pmatrix} a & -b \\ b & a \end{pmatrix}.$$

Then there exist $\lambda_1, \lambda_2 \geq 0$ such that $(\mathbf{A} + p \cdot 1)^{-1} = \lambda_1 1 + \lambda_2 \cdot (\mathbf{A} + p_0 \cdot 1)^{-1}$.

Proof: Since $\mathbf{A} + p \cdot 1$ is invertible, we have that

$$\det(\mathbf{A} + p \cdot 1) = (a+p)^2 + b^2 \neq 0\,.$$

Hence, matrix inversion can be done using Cramer's rule

$$(\mathbf{A} + p \cdot 1)^{-1} = \frac{1}{(a+p)^2 + b^2} \cdot (\mathbf{A}^v + p \cdot 1)\ , \text{ with } \mathbf{A}^v = \begin{pmatrix} a & b \\ -b & a \end{pmatrix}.$$

On the other hand we have

$$\begin{aligned}
(\mathbf{A} + p \cdot 1)^{-1} &= \frac{1}{(a+p)^2 + b^2} (\mathbf{A}^v + p \cdot 1) \\
&= \frac{1}{(a+p)^2 + b^2} (\mathbf{A}^v + p_0 \cdot 1 + (p - p_0) \cdot 1) \\
&= \frac{(a+p_0)^2 + b^2}{(a+p)^2 + b^2} \cdot \frac{1}{(a+p_0)^2 + b^2} (\mathbf{A}^v + p_0 \cdot 1) + \frac{p - p_0}{(a+p)^2 + b^2} \cdot 1 \\
&= \frac{(a+p_0)^2 + b^2}{(a+p)^2 + b^2} \cdot (\mathbf{A} + p_0 \cdot 1)^{-1} + \frac{p - p_0}{(a+p)^2 + b^2} \cdot 1\,.
\end{aligned}$$

Finally, set

$$\lambda_1 = \frac{(a+p_0)^2 + b^2}{(a+p)^2 + b^2} \text{ and } \lambda_2 = \frac{p - p_0}{(a+p)^2 + b^2}\,,$$

each of which is greater than or equal to zero. □

A likewise, but multi-dimensional relationship, can be reduced to Lemma 5.1 by the Sherman-Morrison-Woodbury theorem (Theorem 4.3).

Lemma 5.2 *Let the matrix $\mathbf{A} \in \mathbb{R}^{2n\times 2n}$ be invertible, $\mathbf{U}, \mathbf{V} \in \mathbb{R}^{2\times 2n}$ and also let $0 \leq p_0 \in \mathbb{R}$ such that $\mathbf{A} + p \cdot \mathbf{U}\,\mathbf{V}^\intercal$ is invertible for all $0 \leq p \leq p_0$. Furthermore, assume that both $\mathbf{A}, \mathbf{U}$, and $\mathbf{V}$ are of the form*

$$\begin{pmatrix} \mathbf{A}_1 & -\mathbf{A}_2 \\ \mathbf{A}_2 & \mathbf{A}_1 \end{pmatrix}, \begin{pmatrix} \mathbf{u}_1 & -\mathbf{u}_2 \\ \mathbf{u}_2 & \mathbf{u}_1 \end{pmatrix}, \text{ and } \begin{pmatrix} \mathbf{v}_1 & -\mathbf{v}_2 \\ \mathbf{v}_2 & \mathbf{v}_1 \end{pmatrix},$$

respectively, for $\mathbf{A}_i \in \mathbb{R}^{n\times n}, \mathbf{u}_i, \mathbf{v}_i \in \mathbb{R}^n$. Then there exist $\lambda_1, \lambda_2 \geq 0$ such that

$$\begin{aligned}(\mathbf{A} + p\cdot\mathbf{U}\,\mathbf{V}^\intercal)^{-1} \quad &= \quad \mathbf{A}^{-1} - \lambda_1\mathbf{A}^{-1}\mathbf{U}\,\mathbf{V}^\intercal\mathbf{A}^{-1} \\ &\qquad - \lambda_2\cdot\left(\mathbf{A}^{-1} - (\mathbf{A} + p_0\cdot\mathbf{U}\,\mathbf{V}^\intercal)^{-1}\right).\end{aligned} \tag{24}$$

Proof: One may assume, that p, p_0 are strictly positive, because in either case, $p = 0$ or $p_0 = 0$, Equation 24 is valid for $\lambda_1, \lambda_2 = 0$.

From the Sherman-Morrison-Woodbury theorem (Theorem 4.3) follows

$$(\mathbf{A} + p\cdot\mathbf{U}\,\mathbf{V}^\intercal)^{-1} = \mathbf{A}^{-1} - \mathbf{A}^{-1}\mathbf{U}\left((1/p)1 + \mathbf{V}^\intercal\mathbf{A}^{-1}\mathbf{U}\right)^{-1}\mathbf{V}^\intercal\mathbf{A}^{-1}. \tag{25}$$

Since the matrix $\mathbf{V}^\intercal\mathbf{A}^{-1}\mathbf{U} \in \mathbb{R}^{2\times 2}$, and $1/p < 1/p_0$ match the conditions for matrix and parameter of Lemma 5.1, there exist $\lambda_1, \lambda_2 \geq 0$ such that

$$\left((1/p)1 + \mathbf{V}^\intercal\mathbf{A}^{-1}\mathbf{U}\right)^{-1} = \lambda_1 1 + \lambda_2\cdot\left((1/p_0)1 + \mathbf{V}^\intercal\mathbf{A}^{-1}\mathbf{U}\right)^{-1},$$

which can be applied to Equation 25. We obtain

$$\begin{aligned}&(\mathbf{A} + p\cdot\mathbf{U}\,\mathbf{V}^\intercal)^{-1} = \\ &\mathbf{A}^{-1} - \mathbf{A}^{-1}\mathbf{U}\left(\lambda_1 1 + \lambda_2\cdot\left((1/p_0)\,1 + \mathbf{V}^\intercal\mathbf{A}^{-1}\mathbf{U}\right)^{-1}\right)\mathbf{V}^\intercal\mathbf{A}^{-1} = \\ &\mathbf{A}^{-1} - \lambda_1\mathbf{A}^{-1}\mathbf{U}\,\mathbf{V}^\intercal\mathbf{A}^{-1} - \lambda_2\mathbf{A}^{-1}\mathbf{U}\left((1/p_0)\,1 + \mathbf{V}^\intercal\mathbf{A}^{-1}\mathbf{U}\right)^{-1}\mathbf{V}^\intercal\mathbf{A}^{-1},\end{aligned} \tag{26}$$

which is equal to Equation 24 again by Theorem 4.3. □

Lemma 5.3 *Let $\mathbf{u}_{\mathrm{low}}, \mathbf{v}_{\mathrm{low}}, \mathbf{u}_{\mathrm{up}}, \mathbf{v}_{\mathrm{up}} \in \mathbb{R}^{2\,n}$ be vectors, defining fill-in patterns as in Equation 22. Furthermore, let $\mathbf{A}_0 \in \mathbb{R}^{2\,n\times 2\,n}$ be an invertible matrix arising from a real representation.*

If at least one of $\mathbf{A}_0 + \overline{p}\cdot\mathbf{u}_{\mathrm{low}}\cdot\mathbf{v}_{\mathrm{low}}^\intercal$ or $\mathbf{A}_0 + \overline{p}\cdot\mathbf{u}_{\mathrm{up}}\cdot\mathbf{v}_{\mathrm{up}}^\intercal$ is invertible, then there exists $\lambda \in \mathbb{R}$ such that

$$\begin{aligned}\tfrac{1}{2}\,(\mathbf{A}_0 + \overline{p}\,\mathbf{u}_{\mathrm{low}}\mathbf{v}_{\mathrm{low}}^\intercal)^{-1} + \left(\mathbf{A}_0 + \overline{p}\,\mathbf{u}_{\mathrm{up}}\mathbf{v}_{\mathrm{up}}^\intercal\right)^{-1} = \\ \mathbf{A}_0^{-1} - \lambda\mathbf{A}_0^{-1}\left(\mathbf{u}_{\mathrm{low}}\mathbf{v}_{\mathrm{low}}^\intercal + \mathbf{u}_{\mathrm{up}}\mathbf{v}_{\mathrm{up}}^\intercal\right)\mathbf{A}_0^{-1}.\end{aligned} \tag{27}$$

In case that the regularity can be established for all $p \in [0, \overline{p}]$, λ is strictly positive.

Proof: First, note that Equation 23 yields $\mathbf{v}_{\mathrm{low}}^\intercal\mathbf{A}^{-1}\mathbf{u}_{\mathrm{low}} = \mathbf{v}_{\mathrm{up}}^\intercal\mathbf{A}^{-1}\mathbf{u}_{\mathrm{up}}$. Using

$$\lambda = \frac{1}{2}\frac{\overline{p}}{1 + \overline{p}\,\mathbf{v}_{\mathrm{low}}^\intercal\mathbf{A}^{-1}\mathbf{u}_{\mathrm{low}}} = \frac{1}{2}\frac{\overline{p}}{1 + \overline{p}\,\mathbf{v}_{\mathrm{up}}^\intercal\mathbf{A}^{-1}\mathbf{u}_{\mathrm{up}}} \tag{28}$$

Equation 27 follows from application of Sherman-Morrison to each summand of the left-hand side. The positivity of λ is a consequence of the fact that the denominator $1 + p\,\mathbf{v}_{\mathrm{up}}^{\mathsf{T}}\mathbf{A}^{-1}\mathbf{u}_{\mathrm{up}}$ must not be zero for all p between 0 and $\overline{p}$. $\square$

Finally, we can prove a complex version of Theorem 4.4.

Theorem 5.4 *Let $\mathbf{u}_{\mathrm{low}}, \mathbf{v}_{\mathrm{low}}, \mathbf{u}_{\mathrm{up}}, \mathbf{v}_{\mathrm{up}} \in \mathbb{R}^{2n}$ be vectors, such that the conditions of Equation 23 hold. Furthermore, let $\mathbf{A}_0 \in \mathbb{R}^{2n\times 2n}$ be a matrix arising from a real representation.*

If $\mathbf{A}(p_{\mathrm{low}}, p_{\mathrm{up}}) = \mathbf{A}_0 + p_{\mathrm{low}} \cdot \mathbf{u}_{\mathrm{low}} \cdot \mathbf{v}_{\mathrm{low}}^{\mathsf{T}} + p_{\mathrm{up}} \cdot \mathbf{u}_{\mathrm{up}} \cdot \mathbf{v}_{\mathrm{up}}^{\mathsf{T}}$ is invertible for all $p_{\mathrm{low}} \in [\underline{p}, \overline{p}]$ and $p_{\mathrm{up}} \in [\underline{p}, \overline{p}]$, then the inverse $\mathbf{A}(p,p)^{-1}$ varies in

$$\operatorname{conv}\left(\mathbf{A}(\underline{p},\underline{p})^{-1}; \quad \mathbf{A}(\overline{p},\overline{p})^{-1}; \quad \frac{1}{2}\left(\mathbf{A}(\underline{p},\overline{p})^{-1} + \mathbf{A}(\overline{p},\underline{p})^{-1}\right)\right) .$$

Proof: In order to simplify notation, one may assume that $\underline{p} = 0$ and define

$$\mathbf{A}(p)^{-1} = \mathbf{A}(p,p)^{-1} \quad \text{and} \quad \mathbf{A}_{1/2} = \frac{1}{2}\left(\mathbf{A}(\underline{p},\overline{p})^{-1} + \mathbf{A}(\overline{p},\underline{p})^{-1}\right) . \tag{29}$$

Since one can always find $\mathbf{U}$ and $\mathbf{V}$ fitting into the conditions of Lemma 5.2, such that $\mathbf{U}\mathbf{V}^{\mathsf{T}} = \mathbf{u}_{\mathrm{low}}\mathbf{v}_{\mathrm{low}}^{\mathsf{T}} + \mathbf{u}_{\mathrm{up}}\mathbf{v}_{\mathrm{up}}^{\mathsf{T}}$, that lemma can be combined with Lemma 5.3. Hence, there exist $\lambda_1, \lambda_2 \geq 0$ such that

$$\mathbf{A}(p)^{-1} = \mathbf{A}_0^{-1} + \lambda_1 \cdot \left(\mathbf{A}_{1/2}^{-1} - \mathbf{A}_0^{-1}\right) + \lambda_2 \cdot \left(\mathbf{A}(\overline{p})^{-1} - \mathbf{A}_0^{-1}\right) . \tag{30}$$

On the other hand, $\mathbf{A}(p) = \mathbf{A}(\overline{p}) - (\overline{p} - p) \cdot \mathbf{U}\mathbf{V}^{\mathsf{T}}$ can also be constructed. Thus, we have non-negative μ_1, μ_2 with

$$\mathbf{A}(p)^{-1} = \mathbf{A}(\overline{p})^{-1} + \mu_1 \cdot \left(\mathbf{A}_{1/2}^{-1} - \mathbf{A}(\overline{p})^{-1}\right) + \mu_2 \cdot \left(\mathbf{A}_0^{-1} - \mathbf{A}(\overline{p})^{-1}\right) . \tag{31}$$

Inspecting linear combinations of Equation 30 and 31 show that $\mathbf{A}(p)^{-1}$ lies in the desired convex set. $\square$

We can immediately generalize Theorem 5.4 for the case of several parameters. For illustration consider the real representation $\mathbf{A}(p_1, p_2, p_1, p_2)$ of a complex-valued linear matrix in fill-in pattern form, which depends on two uncertain parameters $p_1 \in [\underline{p}_1, \overline{p}_1]$ and $p_2 \in [\underline{p}_2, \overline{p}_2]$. If $\mathbf{A}(p_1, p_2, p_1, p_2)$ is invertible for all p_1, p_2, we have that

$$\mathbf{A}(p_1, p_2, p_1, p_2)^{-1} \cdot \mathbf{b} \in \operatorname{conv}(\mathbf{x}_1,\ \mathbf{x}_2,\ \mathbf{x}_{1/2})$$

with

$$\begin{aligned}
\mathbf{x}_1 &= \mathbf{A}(\underline{p}_1, p_2, \underline{p}_1, p_2)^{-1} \cdot \mathbf{b} \\
\mathbf{x}_2 &= \mathbf{A}(\overline{p}_1, p_2, \overline{p}_1, p_2)^{-1} \cdot \mathbf{b} \\
\mathbf{x}_{1/2} &= \frac{1}{2} \cdot \Big(\mathbf{A}(\underline{p}_1, p_2, \overline{p}_1, p_2)^{-1} + \mathbf{A}(\overline{p}_1, p_2, \underline{p}_1, p_2)^{-1} \Big) \cdot \mathbf{b}
\end{aligned}$$

by Theorem 5.4. Invoking the procedures again with respect to p_2 for each

$$\mathbf{x} \in \{\mathbf{x}_1, \mathbf{x}_2, \mathbf{x}_{\frac{1}{2}}\},$$

we obtain that

$$\mathbf{A}(p_1, p_2, p_1, p_2)^{-1} \cdot \mathbf{b} \in \operatorname{conv} \Big(\mathbf{x}_{1,1},\ \mathbf{x}_{1,2},\ \mathbf{x}_{1,\frac{1}{2}},\ \mathbf{x}_{2,1},\ \mathbf{x}_{2,2},\ \mathbf{x}_{2,\frac{1}{2}},\ \mathbf{x}_{1/2,1},\ \mathbf{x}_{\frac{1}{2},2},\ \mathbf{x}_{\frac{1}{2},\frac{1}{2}} \Big)$$

with

$$\begin{aligned}
\mathbf{x}_{1,1} &= \mathbf{A}(\underline{p}_1, \underline{p}_2, \underline{p}_1, \underline{p}_2)^{-1} \cdot \mathbf{b} \\
\mathbf{x}_{1,2} &= \mathbf{A}(\underline{p}_1, \overline{p}_2, \underline{p}_1, \overline{p}_2)^{-1} \cdot \mathbf{b} \\
\mathbf{x}_{1,\frac{1}{2}} &= \frac{1}{2} \cdot \Big(\mathbf{A}(\underline{p}_1, \underline{p}_2, \underline{p}_1, \overline{p}_2)^{-1} + \mathbf{A}(\underline{p}_1, \overline{p}_2, \underline{p}_1, \underline{p}_2)^{-1} \Big) \cdot \mathbf{b} \\
\\
\mathbf{x}_{2,1} &= \mathbf{A}(\overline{p}_1, \underline{p}_2, \overline{p}_1, \underline{p}_2)^{-1} \cdot \mathbf{b} \\
\mathbf{x}_{2,2} &= \mathbf{A}(\overline{p}_1, \overline{p}_2, \overline{p}_1, \overline{p}_2)^{-1} \cdot \mathbf{b} \\
\mathbf{x}_{2,\frac{1}{2}} &= \frac{1}{2} \cdot \Big(\mathbf{A}(\overline{p}_1, \underline{p}_2, \overline{p}_1, \overline{p}_2)^{-1} + \mathbf{A}(\overline{p}_1, \overline{p}_2, \overline{p}_1, \underline{p}_2)^{-1} \Big) \cdot \mathbf{b} \\
\\
\mathbf{x}_{\frac{1}{2},1} &= \frac{1}{2} \cdot \Big(\mathbf{A}(\underline{p}_1, \underline{p}_2, \overline{p}_1, \underline{p}_2)^{-1} + \mathbf{A}(\overline{p}_1, \underline{p}_2, \underline{p}_1, \underline{p}_2)^{-1} \Big) \cdot \mathbf{b} \\
\mathbf{x}_{\frac{1}{2},2} &= \frac{1}{2} \cdot \Big(\mathbf{A}(\underline{p}_1, \overline{p}_2, \overline{p}_1, \overline{p}_2)^{-1} + \mathbf{A}(\overline{p}_1, \overline{p}_2, \underline{p}_1, \overline{p}_2)^{-1} \Big) \cdot \mathbf{b} \\
\mathbf{x}_{\frac{1}{2},\frac{1}{2}} &= \frac{1}{4} \cdot \Big(\mathbf{A}(\underline{p}_1, \underline{p}_2, \overline{p}_1, \overline{p}_2)^{-1} + \mathbf{A}(\underline{p}_1, \overline{p}_2, \overline{p}_1, \underline{p}_2)^{-1} + \\
&\qquad \mathbf{A}(\overline{p}_1, \underline{p}_2, \underline{p}_1, \overline{p}_2)^{-1} + \mathbf{A}(\overline{p}_1, \overline{p}_2, \underline{p}_1, \underline{p}_2)^{-1} \Big) \cdot \mathbf{b}
\end{aligned}$$

The general case is illustrated in Algorithm 3.

Example For instance, Algorithm 3 is explained by analyzing AC equations for the serial circuit of Figure 3. It has the same topological structure as the simple voltage divider of Figure 1, but one of the resistors is replaced by a capacitor. The same is true for the system of equations,

$$\begin{pmatrix} \frac{1}{R_1} & -\frac{1}{R_1} & 1 \\ -\frac{1}{R_1} & \frac{1}{R_1} + C_1\, s & 0 \\ 1 & 0 & 0 \end{pmatrix} \cdot \begin{pmatrix} V_1 \\ V_2 \\ I_{V_0} \end{pmatrix} = \begin{pmatrix} 0 \\ 0 \\ V_0 \end{pmatrix}, \qquad (32)$$

Algorithm 3 Complex-valued linear systems solver

Input: Real representation: $\mathbf{A}(\mathbf{p}, \mathbf{p}) \in \mathbb{R}^{2n\times 2n}$, $\mathbf{b} \in \mathbb{R}^{2n}$, and $\mathbf{p} \in [\mathbf{p}] \in [\mathbb{R}]^{n_\mathbf{p}}$
Output: $R = \{\mathbf{x}_1, \ldots, \mathbf{x}_{2^{n_\mathbf{p}}}\}$ such that $\mathbf{A}(\mathbf{p}, \mathbf{p})^{-1}\mathbf{b} \subseteq \operatorname{conv}(R)$, for all $\mathbf{p} \in [\mathbf{p}]$

Set $s := \operatorname{sign}(\det \mathbf{A}(\mathbf{p}_0, \mathbf{p}_0))$ for some $\mathbf{p}_0 \in [\mathbf{p}]$.
if $s = 0$ **then**
  return failed
end if
/* Initialize matching sets */
Set $\mathbf{S}_{[\mathbf{p}]} := \{\{(\underline{p}_1, \underline{p}_1)\}, \{(\overline{p}_1, \underline{p}_1)\}, \{(\underline{p}_1, \overline{p}_1), (\overline{p}_1, \underline{p}_1)\}\}$.
for $i = 2, \ldots, n_\mathbf{p}$ **do**
  Set $T := \emptyset$.
  for $S \in \mathbf{S}_{[\mathbf{p}]}$ **do**
    $T = T \cup \left\{\left\{(\mathbf{p}, \underline{p}_i, \mathbf{q}, \underline{p}_i) \,\middle|\, (\mathbf{p}, \mathbf{q}) \in S\right\}, \left\{(\mathbf{p}, \overline{p}_i, \mathbf{q}, \overline{p}_i) \,\middle|\, (\mathbf{p}, \mathbf{q}) \in S\right\}\right\}$
    $T = T \cup \left\{\bigcup_{(\mathbf{p},\mathbf{q})\in S} \left\{(\mathbf{p}, \underline{p}_i, \mathbf{q}, \overline{p}_i), (\mathbf{p}, \overline{p}_i, \mathbf{q}, \underline{p}_i)\right\}\right\}$
  end for
  Set $\mathbf{S}_{[\mathbf{p}]} = T$.
end for
/* Start computations */
Set $R := \emptyset$.
for $S \in \mathbf{S}_{[\mathbf{p}]}$ **do**
  Set $T := \emptyset$.
  for $(\mathbf{p}, \mathbf{q}) \in S$ **do**
    /* Regularity test */
    if $\det \mathbf{A}(\mathbf{p}, \mathbf{q}) \neq s$ **then**
      return failed
    else
      Set $T := T \cup \{(\mathbf{A}(\mathbf{p}, \mathbf{q}))^{-1} \cdot \mathbf{b}\}$
    end if
  end for
  Set $R := R \cup \{\frac{1}{\#(T)} \cdot \sum_{\mathbf{x}\in T} \mathbf{x}\}$
end for
return R

which is to be treated for a constant frequency of $1000\,\mathrm{Hz}$, such that we have complex-valued $s = 2\,\pi\,i \cdot 1000\,\mathrm{s}^{-1}$ with an exact independent voltage source of $V_0 = 1\,\mathrm{V}$, and two tolerance-affected parameters given as $C_1/1\,\mu\mathrm{F} \in [0.8, 1.2]$ and $R_1/1\,\Omega \in [80, 120]$. For analyzing the range using Algorithm 4, 16 linear systems have to be solved. The results can be used to make up the nine points defining the convex set. The range of the current I_{V_0} in the complex range is shown in Figure 4. The smallest rectangle in the complex plane containing all solutions is easily obtained by computing the interval hull of real and imaginary

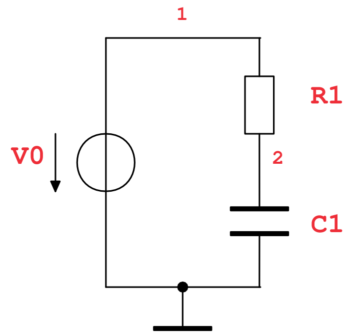

Figure 3 Serial circuit.

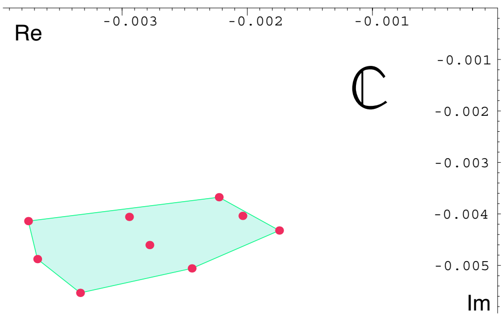

Figure 4 Range of the solution I_{V_0}.

parts of all points such that

$$I_{V_0}/1\,\mathrm{mA} \in [-3.76, -1.73] + i\,[-5.53, -3.68]\,.$$

But we are sometimes interested in the range of the absolute and the phase value of the complex variable. These can be approximately determined computing the respective values over all points. In the example, we obtain

$$\left|I_{V_0}\right|/1\,\mathrm{mA} \in [4.30, 6.46] \text{ and phase } \varphi/1^\circ \in [-132.2, -111.9]\,.$$

Note, that the actual lower bound for the absolute value may be slightly smaller, if a normal vector of the nearest edge of the convex hull meets the origin. For a justification of this problem see [4, Section 3.3.2]. For most practical applications – like the example above – the approximate solution gives sufficiently accurate bounds (see Figure 4). Lower and upper bounds obtained from Algorithm 3 for the frequency response with respect to frequencies from $1\,\mathrm{Hz}$ up to $1\,\mathrm{MHz}$ together with a good (inner) approximation of the range are shown in Figure 5, which results from a sufficiently large number of parameter sweeps. The actual range is perfectly met by the results computed with the method described in this section.

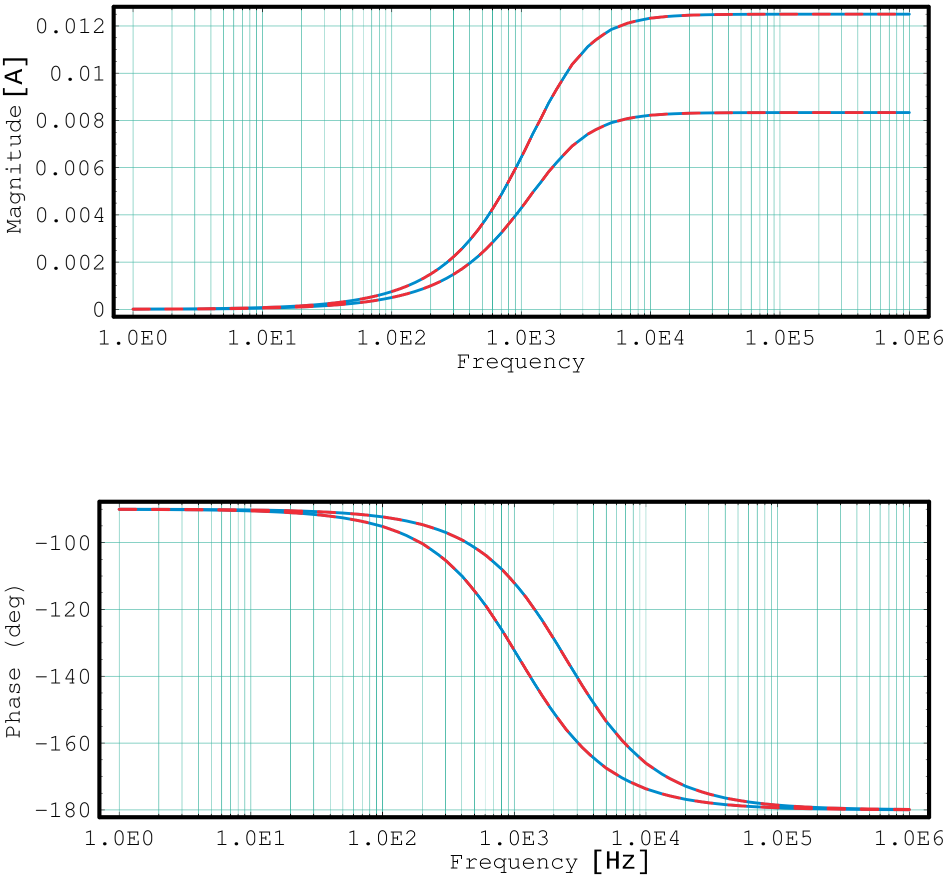

Outer bounds to absolute value and phase of I_{V_0} obtained from Algorithm 3 (red) and parameter sweeps (blue). Figure 5

5.1 A faster approach

Although Theorem 5.4 can easily be generalized to the case of several parameters, it is not the method of choice for practical problems, because it would lead to $2^{2n_\mathbf{p}}$ linear systems to be solved. But in order to avoid such conservative bounds, as obtained by simply using the real representation, a combination with the ideas of the resistive case is suitable. In contrary, Algorithm 2, the quick variant for solving real-valued systems, can easily be applied to a real representation $\mathbf{A}(\mathbf{p}, \mathbf{p})$ with polynomial computational complexity. Unfortunately, this does not treat the dependence of the parameters accurately, because in this case the occurrences of the parameters in the matrix $\mathbf{A}(\mathbf{p}, \mathbf{p})$ do not fit in the scheme of the fill-in pattern form. Hence, the quick procedure actually bounds the solutions $\mathbf{A}(\mathbf{p}, \mathbf{q})^{-1}\mathbf{b}$ for all $\mathbf{p} \in [\mathbf{p}]$ and $\mathbf{q} \in [\mathbf{p}]$.

In order to avoid too conservative bounds, a combination of both approaches is presented in the following. The dependence of $\mathbf{A}(\mathbf{p}, \mathbf{p})$ with respect to a single parameter is given by Theorem 5.4. Therefore, the result $\mathbf{A}(p,p)^{-1} \cdot \mathbf{b}$ lies in

$$\operatorname{conv}\{\mathbf{A}(\underline{p},\underline{p})^{-1} \cdot \mathbf{b},\ \mathbf{A}(\overline{p},\overline{p})^{-1} \cdot \mathbf{b},\ \frac{1}{2}\left(\mathbf{A}(\overline{p},\underline{p})^{-1} + \mathbf{A}(\underline{p},\overline{p})^{-1}\right) \cdot \mathbf{b}\}\,, \tag{33}$$

for $p \in [\underline{p},\overline{p}]$. As mentioned in above there exist vectors $\mathbf{u}_{\text{up}}, \mathbf{v}_{\text{up}}, \mathbf{u}_{\text{low}}$, and $\mathbf{v}_{\text{low}} \in \mathbb{R}^{2\,n}$, with

$$\mathbf{u}_{\text{low}} = \mathbf{u}_{\text{up}} \cdot \begin{pmatrix} 0 & -1 \\ 1 & 0 \end{pmatrix} \text{ and } \mathbf{v}_{\text{low}} = \mathbf{v}_{\text{up}} \cdot \begin{pmatrix} 0 & -1 \\ 1 & 0 \end{pmatrix} \tag{34}$$

such that

$$\mathbf{A}(p,q) = \mathbf{A}(\underline{p},\underline{p}) + (p-\underline{p}) \cdot \mathbf{u}_{\text{up}}\,{\mathbf{v}_{\text{up}}}^{\mathsf{T}} + (q-\underline{p}) \cdot \mathbf{u}_{\text{low}}\,{\mathbf{v}_{\text{low}}}^{\mathsf{T}}\,. \tag{35}$$

Hence, the matrix $\mathbf{A}(p,q)$ is a matrix in fill-in pattern form with respect to the parameters p and q. Hence, we can try to use the Sherman-Morrison formula to compute the points

$$\mathbf{A}(\underline{p},\underline{p})^{-1} \cdot \mathbf{b},\ \mathbf{A}(\underline{p},\overline{p})^{-1} \cdot \mathbf{b},\ \mathbf{A}(\overline{p},\underline{p})^{-1} \cdot \mathbf{b},\ \mathbf{A}(\overline{p},\overline{p})^{-1} \cdot \mathbf{b}\,,$$

which are needed to bound the solution set accurately by Theorem 5.4. Starting at the point $(\underline{p},\underline{p})$, we compute

$$\tilde{\mathbf{b}} = \mathbf{A}(\underline{p},\underline{p})^{-1} \cdot \mathbf{b} \text{ and } \tilde{\mathbf{u}}_{\text{up}} = \mathbf{A}(\underline{p},\underline{p})^{-1} \cdot \mathbf{u}\,.$$

As a consequence of Equation 34, the analogously defined vector $\tilde{\mathbf{u}}_{\text{low}}$ is simply given by

$$\tilde{\mathbf{u}}_{\text{low}} = \tilde{\mathbf{u}}_{\text{up}} \cdot \begin{pmatrix} 0 & -1 \\ 1 & 0 \end{pmatrix}\,.$$

Now, let $\Delta p := \overline{p} - \underline{p}$, and set

$$d := \frac{1}{\Delta p} + \left(\mathbf{v}_{\text{up}}^{\mathsf{T}} \cdot \tilde{\mathbf{u}}_{\text{up}}\right)\,.$$

If $d > 0$, then the condition for the application of the Sherman-Morrison formula is fulfilled. Hence, we may calculate

$$\mathbf{b}^*_{\text{up}} := \mathbf{A}(\overline{p},\underline{p})^{-1} \cdot \mathbf{b} \quad = \quad \tilde{\mathbf{b}} - \frac{1}{d}\,\tilde{\mathbf{u}}_{\text{up}} \cdot \left(\tilde{\mathbf{v}}_{\text{up}}^{\mathsf{T}} \cdot \tilde{\mathbf{b}}\right) \tag{36}$$

and analogously $\mathbf{b}^*_{\text{low}}$ and $\mathbf{u}^*_{\text{low}}$. Consequently, one can compute:

$$\frac{1}{2} \cdot \left(\mathbf{b}^*_{\text{up}} + \mathbf{b}^*_{\text{low}}\right) = \tilde{\mathbf{b}} - \frac{1}{2\,d} \cdot \left(\tilde{\mathbf{u}}_{\text{up}} \cdot \left(\tilde{\mathbf{v}}_{\text{up}}^{\mathsf{T}} \cdot \tilde{\mathbf{b}}\right) + \tilde{\mathbf{u}}_{\text{low}} \cdot \left(\tilde{\mathbf{v}}_{\text{low}}^{\mathsf{T}} \cdot \tilde{\mathbf{b}}\right)\right)\,. \tag{37}$$

Finally, we have to calculate $\mathbf{A}(\overline{p},\overline{p})^{-1} \cdot \mathbf{b}$. This is similar to the application of Algorithm 2 to a real-valued system with two parameters. For abbreviation define

$$d^* := \frac{1}{\Delta p} + \left(\mathbf{v}_{\text{low}}^{\mathsf{T}} \cdot \mathbf{u}^*_{\text{low}}\right)\,. \tag{38}$$

If $d^* > 0$ we can apply Sherman-Morrison a second time, such that

$$\mathbf{A}(\overline{p},\overline{p})^{-1} \cdot \mathbf{b} = \mathbf{b}^*_{\text{up}} - \frac{1}{d^*}\, \mathbf{u}^*_{\text{low}} \cdot \left(\tilde{\mathbf{v}}^{\mathsf{T}}_{\text{low}} \cdot \mathbf{b}^*_{\text{up}}\right) . \tag{39}$$

Algorithm 4 Quick complex-valued linear system solver

Input: Real representation: $\mathbf{A}(\mathbf{p}) = \mathbf{A}_0 + \sum_{i=1}^{n_\mathbf{p}} p_i \left(\mathbf{u}_{\text{up},i} \cdot \mathbf{v}^{\mathsf{T}}_{\text{up},i} + \mathbf{u}_{\text{low},i} \cdot \mathbf{v}^{\mathsf{T}}_{\text{low},i}\right) \in \mathbb{R}^{2n\times 2n}$, $\mathbf{b} \in \mathbb{R}^n$, and $\mathbf{p} \in [\mathbf{p}] \in [\mathbb{R}]^{n_\mathbf{p}}$
Output: $[\mathbf{x}] \supseteq \mathbf{A}(\mathbf{p})^{-1}\mathbf{b}$, for all $\mathbf{p} \in [\mathbf{p}]$

```
for i := 1, ..., n_p do
   Set Δp_i := p̄_i − p_i.
   Set [ũ_i] := A_0^{-1} · u_up,i.
end for
Set [ũ_{n_p+1}] := A_0^{-1} · b
Set S := {[ũ_i] | i = 1, ..., n_p + 1}.
for i = 1, ..., n_p do
   S := S \ {[ũ_i]}
   Set [ũ_low,i] := [ũ_i] · ( 0 −1 ; 1 0 )
   Set [d] := 1/Δp_i + (v^T_up,i · [ũ_i]).
   /* Regularity test */
   if [d] > 0 then
      Set [u*_i] = (1 − (v^T_up,i · [ũ_i]) / [d]) [ũ_low,i].
      Set [d*] := 1/Δp_i + (v^T_low,i · [u*_i]).
      if [d*] > 0 then
         for [ũ] ∈ S do
            Set [Δũ] := [ũ_i] (v^T_up,i · [ũ]).
            [u*] := [ũ] − [Δũ]/[d]
            [ũ] := [{[ũ], [ũ] − ([Δũ] + [ũ_low,i](v^T_low,i · [ũ])) / (2[d]), [u*] − ([u*_i](v^T_low,i · [u*])) / [d*]}]
         end for
      else
         return failed
      end if
   else
      return failed
   end if
end for
[x] := [ũ_{n_p+1}]
```

In order to treat several parameters, we can now move from sets of real-valued vectors to boxes like in Algorithm 2. This is done by replacing the convex hull by the interval hull in Equation 33. As seen in the derivation of Algorithm 2, the vectors $[\tilde{\mathbf{u}}_i]$ have to be updated with respect to to each parameter in the same manner like the right-hand side vector $\mathbf{b}$. The procedure is summarized in Algorithm 4. Like for Algorithm 2 the loss of accuracy due to wrapping intermediate results by the interval hull pays off by reducing the computational complexity order to $n_{\mathbf{p}}^2$.

Example We now apply Algorithm 4 to the real representation of Equation 32 for the same data as above, i. e. for constant frequency of $1000\,\mathrm{Hz}$, such that we have $s = 2\,\pi\,i \cdot 1000\,\mathrm{s}^{-1}$, with an exact independent voltage source of $V_0 = 1\,\mathrm{V}$, and two tolerance affected parameters given as

$$C_1/1\,\mu\mathrm{F} \in [0.8, 1.2] \text{ and } R_1/1\,\Omega \in [80, 120]\,.$$

Again, we have to deal with a reciprocal parameter $\frac{1}{R_1}$, whose range is then the interval $[0.0083, 0.0125]$. Since we deal with constant frequency, we can interprete of the expression

$$C_1\,2\boldsymbol{n}\pi f \in [0.8\,10^{-6}, 1.2\,10^{-6}] \cdot 2\,\pi\,1000 = [0.005, 0.0076]$$

as an parameter. Application of the algorithm leads to bounds for the current

$$I_{V_0}/1\,\mathrm{mA} \in [-4.27, -1.73] + i\,[-5.56, -3.68]\,,$$

which properly includes the rectangle $[-3.76, -1.73] + i\,[-5.53, -3.68]$, computed using Algorithm 2.

The response for the frequencies from $1\,\mathrm{Hz}$ up to $1\,\mathrm{MHz}$ is compared to the results from Algorithm 3 in Figure 6. The curves denoting lower and upper bounds for both computations, respectively, indicate similar qualitative behavior. Although the results obtained from Algorithm 4 are less accurate, they afford to draw conclusions about the performance of the circuit.

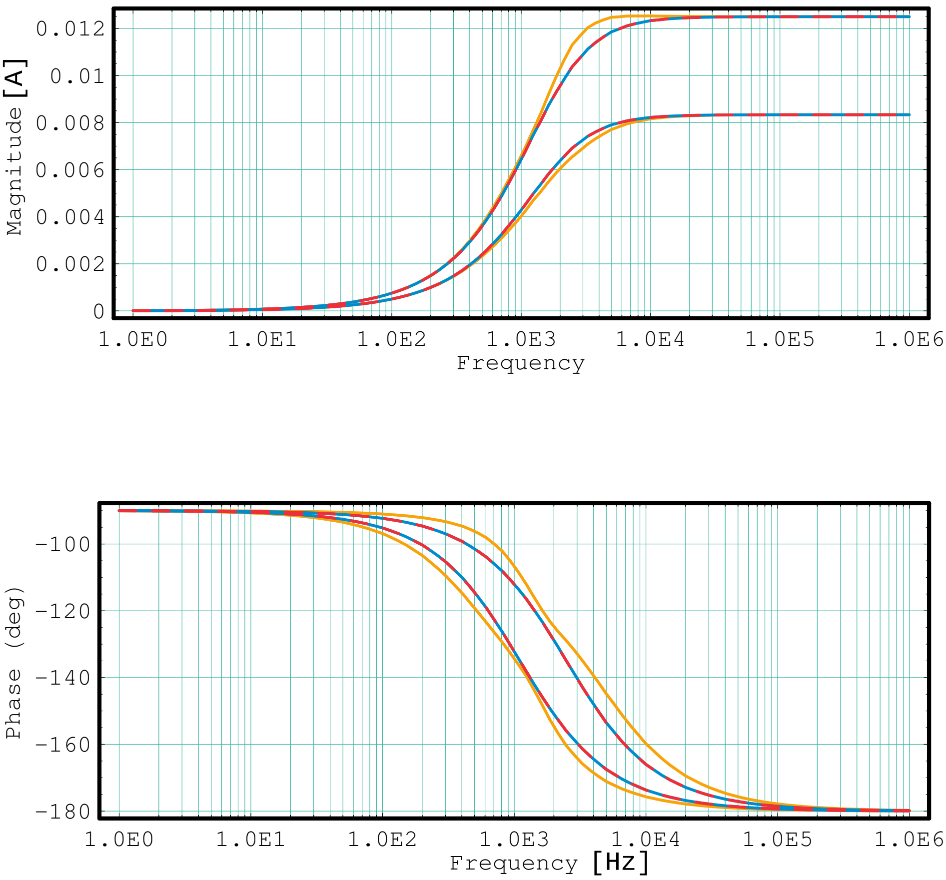

Outer bounds obtained using Algorithm 3 (solid orange), and Algorithm 4 (dashed). Figure 6

6 Implementations and Applications

In this section, we apply the implementations of the algorithms to practical examples. The main goal, besides the development of interval solvers, which are tuned to solve problems from analog circuit design, was to implement the resulting algorithms. This was done as an extension to the electronic design tool Analog Insydes on the basis of the computer algebra system Mathematica [17].

The selection of the example applications was motivated in the following way:

The analysis of a *tone controller* is the first example circuit. The output characteristic is computed with respect to uncertain resistances and capacitances. The result can be used for sizing the potentiometers, which control the amplification of low and high frequencies, because we can compute the worst case values of minimal and maximal amplification.

Secondly, the ability of the interval-valued AC analysis to treat real-world circuits is discussed with respect to an *operational amplifier*. It contains a large number of components and cannot be treated with classical interval methods.

The example calculations below have been computed under SuSE-Linux 9.0-i586 on an Intel Xeon™ $3\,\mathrm{GHz}$ dual-processor machine with four gigabytes of RAM, using Mathematica 4.2 and a developer version of Analog Insydes.

6.1 Implementations

Before discussing a few example applications in detail, we first give a brief description of the Analog Insydes commands, which are necessary to carry out the example calculations. For a more extensive treatment of Analog Insydes see [18]. We will concentrate on main issues, which are important for the treatment of the examples in this section. In particular, the procedures of the interval solvers are presented. These have been implemented as an extension to Analog Insydes on the basis of Mathematica. We will assume, that the reader is familiar with the basic Mathematica syntax. See [17] for an introduction to Mathematica.

The procedures for solving interval-valued problems are actually implementations of the newly introduced algorithms. The functions were set up in such a way, that they fit in the structure of the existing Analog Insydes routines. It was also attached importance to the usability and computation speed of the procedures. Obviously, interval algorithms still last longer than calculations using floating-point solvers, but at least for linear problems, these can be solved in reasonable time.

Data structures Analog Insydes uses a special data structure to store a symbolic system of equations. It contains the equations and variables together with additional information, like the design point. A **`DAEObject`** has the following structure:

`DAEObject[`*mode***`][{`***eqs***`,`** *vars***`}, {`***options***`}]`**

The value of *mode* shows, whether the **`DAEObject`** corresponds to a static, frequency domain, or transient analysis. The field *options* contains user-accessible information about the object.

In addition, the interval-solver extension carries a new object for marking terms in an expression. The **`TermMarkerObject`** includes the marked term, the variables of the term, and an additional symbol, which can be used to uniquely identify the object.

`TermMarkerObject[`*term***`,`***marker***`,{`***vars***`}][`***vars***`]`**

The **`TermMarkerObject`** respects derivation and evaluates to *term*, if *term* is a real or interval value. It is instantiated by the command

`MarkTerm[`*term***`,`***marker***`,`***symbs***`]`** ,

where *symbs* denotes a variable or a list of variables. It is currently used to mark nonlinear terms in interval models, which can easily be detected by the interval routines. Another type of object, which will occur during the calculations of this section is the **`DataObject`**, which is a container for the numerical results obtained from functions of Analog Insydes and the interval-solver extension.

Tolerance specifications Yet, the **`DAEObject`** does not contain information about the component tolerances. Hence, these have to be stated separately. A tolerance specification is usually given as a list, whose elements are rules of the form :

param $\rightarrow$ *val* .

The tolerance values *val* may be the symbol **`Automatic`**, intervals, or real numbers, where intervals directly state the parameter range, and a real number ε yields the interval

$$[1-\varepsilon, 1+\varepsilon]\cdot r\,,$$

where $r \in \mathbb{R}$ is given by the design point. Furthermore, if *val* is set to **`Automatic`** a standard value for ε is used. This value can be changed using the option setting **`Tolerance`** $\rightarrow$ *value* of the interval solvers. The right-hand side values are assigned to the symbolic parameters matching the expression *param*, which may be a symbol or a string pattern. For instance, **`R1`** matches only the element **`R1`**, but **`"R*"`** corresponds to all parameters, whose parameter names begin with the letter 'R'.

Linear interval solvers For an efficient frequency-response (AC) analysis of tolerance-affected analog circuits the algorithms of Section 4 are implemented. The interval-based tolerance analysis is invoked by **`IntervalACAnalysis`**. The syntax of the command is close to the one of the corresponding Analog Insydes command **`ACAnalysis`**, but with tolerance specifications added.

`IntervalACAnalysis[`*dae***`,{`***fvar, fstart, fend***`},{`***tolerance-specs***`}`**⟨**`,`***opts*⟩**`]`**

The frequency variable is selected by *fvar*, and start and end frequencies are defined by *fstart* and *fend*, respectively. The underlying interval solver may be selected by adding optional arguments to *opts*.

The setting **`Method`** → **`MonotonicACAnalysis`** switches to Algorithm 3, while **`Method`** → **`QuickACAnalysis`** calls an implementation of Algorithm 4. Also, a reference implementation of Rohn's almost classical sign-accord method can be selected using **`Method`** → **`SignAccordACAnalysis`** [19]. The command returns a list of two objects, which are generated from the interval results. By default, these contain information about the curves corresponding to the values $a_{\min} \cdot e^{i\,\varphi_{\min}}$ and $a_{\max} \cdot e^{i\,\varphi_{\max}}$ for each frequency and variable. The values $a_{\min}$ and $a_{\max}$ denote the minimal and maximal absolute values of the complex-valued result, whereas $\varphi_{\min}$ and $\varphi_{\max}$ give the range of the phase. The latter are chosen, such that $\varphi_{\max} - \varphi_{\min}$ is minimal. The way how the curves are computed from the raw interval data, can be controlled by the user using the option **`PostProcessingFunction`**. The number of frequency values per decade to be treated can be controlled by adding

`PointsPerDecade` → *ppd*

to the option sequence. For **`MonotonicACAnalysis`** only, one can switch to Analog Insydes' upcoming fast numerical solvers using the setting

`UseExternals` → **`True`**.

6.2 AC Analysis of a Tone-Control Circuit

Our next goal is to analyze a tone-control circuit. This filter can be used to control the amplification of low and high frequencies independently, whereas the mid-frequency stays constant [20]. A common realization is shown in Figure 7. The magnitude can be lowered or raised with two pre-set potentiometers. We are interested in the small-signal behavior for the extremal settings of the potentiometers, when both are set to maximal and minimal respectively. Now, Algorithm 2 can be used to compute sufficiently tight bounds for the frequency response. A Bode diagram of the results with respect to a tolerance of 5% for the output voltage is illustrated in Figure 8.

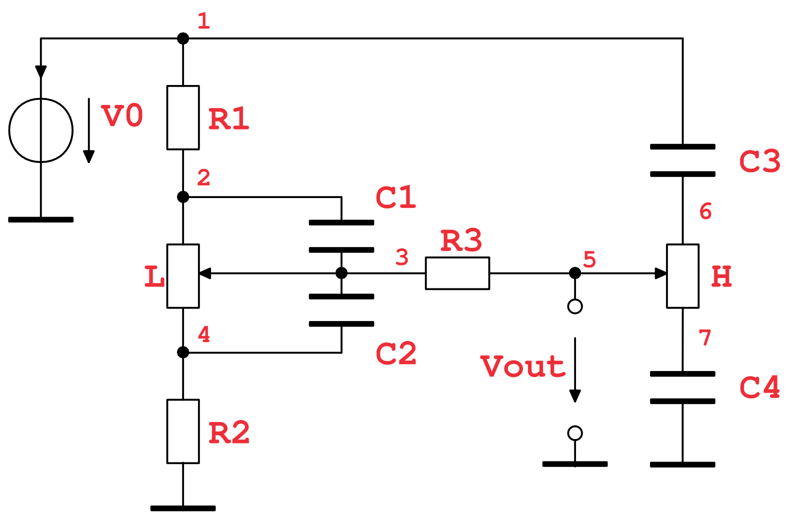

Schematics of a tone-control circuit. Figure 7

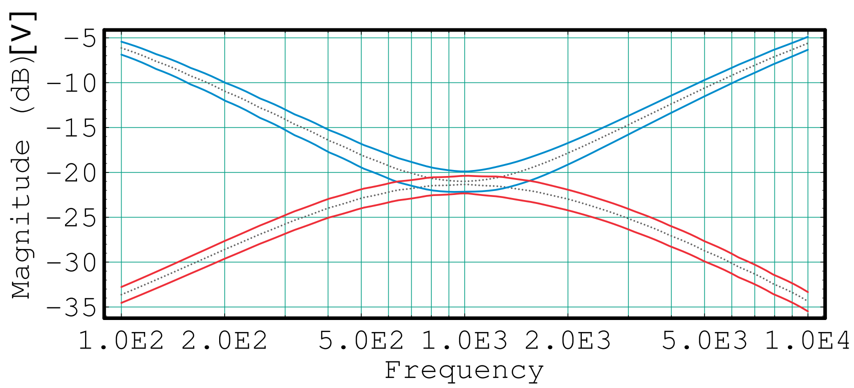

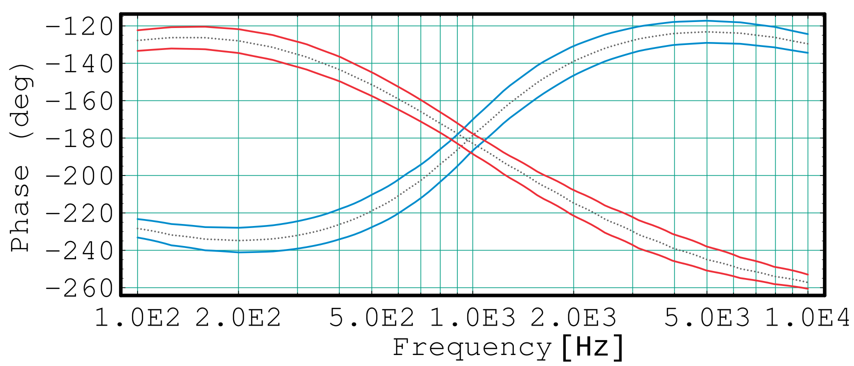

Outer bounds for extremal potentiometer settings (blue/red), and original design point (dotted). Figure 8

The computation for twenty points in the frequency domain from $100\,\mathrm{Hz}$ to $10\,\mathrm{kHz}$ needs 3.05 seconds. In contrary, a simple parameter sweep with three points per parameter yields a computation time of 35.22 seconds. It is also possible to obtain slightly sharper bounds using Algorithm 1, where the use of Analog Insydes' fast external routines is switched on. But for this approach $2^{14} = 16384$ corner points have to be treated, which lasts more than one hour and needs about two gigabytes of RAM.

Here, interval analysis delivers guaranteed lower bounds to the maximal and upper bounds to the lower amplification, respectively. Hence, one can determine with mathematical certainty, whether the ranges of the potentiometers are chosen large enough to obtain the desired output voltages.

6.3 AC Analysis of an Operational Amplifier

In this section we demonstrate the ability of Algorithm 2 to treat real-world examples. We consider the operational amplifier, whose schematics can be found in Figure 9. The small-signal behavior of the transistors is modeled by the linear circuit of Figure 10, which consists of resistors, capacitors, and controlled sources.

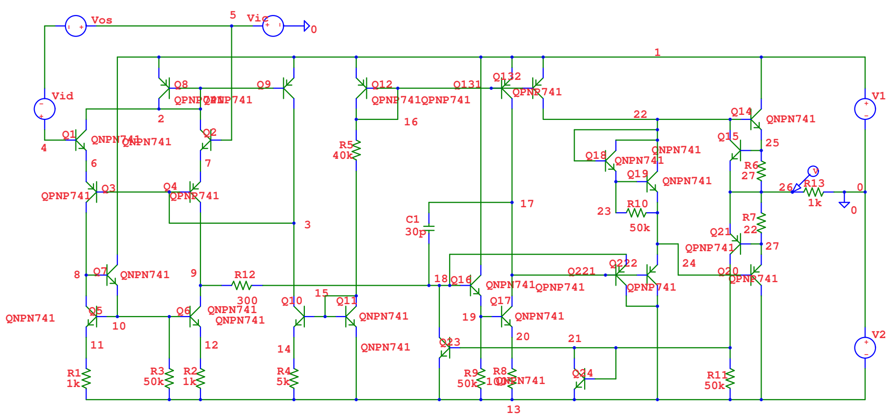

Figure 9 Schmematics of the operational amplifier $\mu A741$.

Since this equivalent circuit diagram is only valid for a constant operating point, we will only vary such circuit elements, that do not change the operating point. Hence, we assign tolerances of 20% to the capacitance values.

Then an interval-valued AC analysis is performed for 70 frequency values between $0.1\,\mathrm{Hz}$ and $1\,\mathrm{MHz}$ in eleven minutes and 47 seconds. The frequency response of the output voltage at node 26 is presented in Figure 11. We obtain

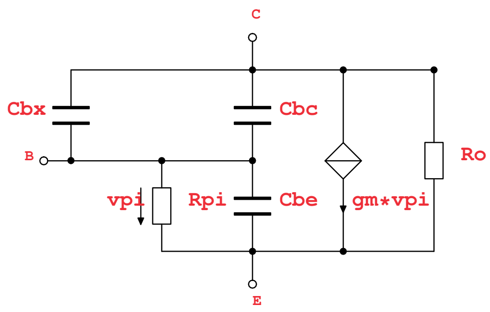

Simplified equivalent circuit schematics of a bipolar-junction transistor.

Figure 10

interpretable results: upper und lower bounds are very close to the curve, which corresponds to the original design point.

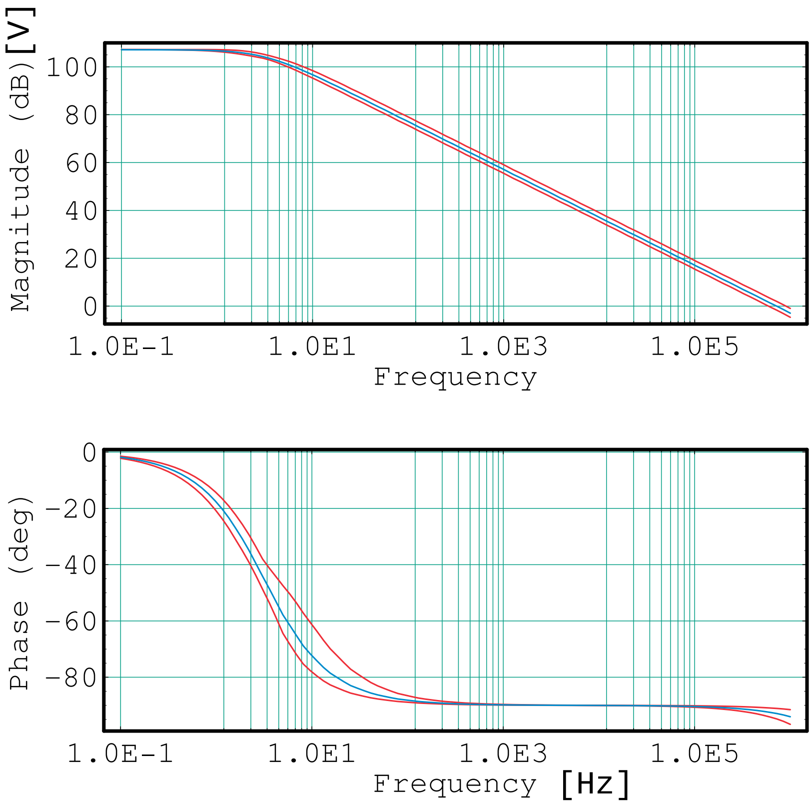

Outer bounds (red), and frequency response with respect to original design point (blue).

Figure 11

7 Conclusions

The methods described above were implemented as an extension to the toolbox *Analog Insydes* [16, 18], an add-on package to the computer algebra system *Mathematica* [17] for modeling, analysis, and design of analog circuits.

The techniques can be used to obtain meaningful bounds to the simulation results of analog circuits with uncertain parameters. As opposed to earlier attempts to use interval arithmetic in this area, which were restricted to the sparse tableau formulation, the dependence between parameters with multiple occurrences is treated explicitely.

For efficient implementation, it is crucial to regard possible dependencies in circuit equations. Part and parcel of of this strategy is the handling of fill-in patterns for those parameters related to uncertain components. These patterns arise from linear circuit analysis, where they are used for efficient equation setup. With a view towards the incorporation of the methods in the industrial design flow, procedures were presented, which are capable of the treatment of a large number of tolerance-affected components.

First of all, the application of interval analysis to analog circuits has been motivated. For this purpose, we have given a brief description of tolerance-related issues in circuit design. It has been mentioned, why intervals occur in a natural manner. Also, major drawbacks for the application of classical interval methods in this context have been pointed out. After stating preceding numerical and interval-based approaches for tolerance analysis, the main targets of this work have been specified.

Secondly, a short introduction to interval arithmetic and derived algorithms has been given. This includes the treatment of very basic notations and properties, as well as previous algorithms for solving interval-valued systems of equations and some implementation notes. Also, we have described the dependency problem, which causes very conservative bounds to the solution sets.

It has been proven, that for circuits consisting of linear elements these result in matrix equations in fill-in pattern form with respect to tolerance-affected component parameters. This special matrix structure can be used for utilizing monotonic properties of the solution set, which is crucial for efficient solving of the linear system.

But still, this restricts interval analysis to the treatment of small circuits. In order to tackle this problem, a special solver for linear systems in fill-in pattern form has been designed in Section 4. This involved the Sherman-Morrison formula in two ways: On the one hand, it has been used to prove monotony properties of the solutions, on the other hand repeated application of the formula gives a constructive way for computing sufficiently tight bounds. The latter is of quadratic complexity in the number of interval-valued parameters. This approach has also been extended to complex-valued systems emerging from small-signal analysis of linear circuits. In addition, an alternative algorithm has been presented, which can be used to compute close bounds to the variance of the results in the complex plane.

The algorithms shown in this paper have been implemented and integrated in the framework of the circuit analysis tool Analog Insydes. The implementation is concisely documented and tested in Section 6. The performance of the new methods has been demonstrated for a frequency response analysis of a tone-control circuit and a real-world operational amplifier. It illustrates that the linear methods are capable of providing interpretable results for analog circuits of considerable size in suitable time. Since equivalent circuit diagrams are widely used for standard small-signal applications, this finds practical utilization in analog circuit analysis of real-world devices.

References

[1] V. Litkovski and M. Zwolinski. *VLSI Circuit Simulation and Optimization*. Chapman & Hall, London, UK, 1997.

[2] E. R. Hansen. *Global optimization using interval methods*, volume 165 of *Monographs and textbooks in pure and applied mathematics*. Marcel Dekker, New York, 1992.

[3] R. B. Kearfott. *Rigorous Global Search: Continuous Problems*, volume 13 of *Nonconvex optimization and its applications*. Kluwer Academic Publishers, Dordrecht, The Netherlands, 1996.

[4] L. V. Kolev. *Interval Methods for Circuit Analysis*. World Scientific, Singapore, 1993.

[5] J. Vlach and K. Singhal. *Computer Methods for Circuit Analysis and Design*. Van Nostrand Reinhold, New York, 2nd edition, 1993.

[6] Alexander Dreyer. Combination of symbolic and interval-numeric methods for analysis of analog circuits. In *Proc. 8th International Workshop on Symbolic Methods and Applications in Circuit Design (SMACD 2004)*, Wroclaw, Poland, Sep. 2004.

[7] Ashwin Ganesan, Sheila R. Ross, and B. Ross Barmish. An extreme point result for convexity, concavity and monotonicity of parameterized linear equation solutions. *Linear Algebra an its Applications*, 390:61–73, October 2004.

[8] Alexander Dreyer. *Interval Analysis of Analog Circuits with Component Tolerances*. PhD thesis, Kaiserslautern University of Technology, Kaiserslautern, Germany, 2005. Shaker Verlag, Aachen, Germany.

[9] Jochen Werner. *Numerische Mathematik 1*. vieweg, Braunschweig, Germany, 1991.

[10] Jochen Werner. *Numerische Mathematik 2*. vieweg, Braunschweig, Germany, 1992.

[11] Gerhard Zielke. Inversion of modified symmetric matrices. *Journal of the ACM*, 15(3):402–408, July 1968.

[12] Eckhard Hennig. *Symbolic Approximation and Modeling Techniques for Analysis and Design of Analog Circuits*. Shaker Verlag, Aachen, Germany, 2000.

[13] Tim Wichmann. *Symbolische Reduktionsverfahren für nichtlineare DAE-Systeme*. Berichte aus der Mathematik. Shaker Verlag, Aachen, Germany, 2004.

[14] Christos H. Papadimitriou and Kenneth Steiglitz. *Combinatorial optimization: algorithms and complexity*. Prentice Hall, 1982. Papadimitriou.

[15] MicroSim Corporation. *MicroSim PSpice & Basics User's Guide*, 1996.

[16] Fraunhofer ITWM. `http://www.analog-insydes.de`. Analog Insydes website.

[17] S. Wolfram. *The Mathematica Book*, volume 4. Wolfram Media/Cambridge University Press, 4th edition, 1999.

[18] Jochen Broz, Alexander Dreyer, Thomas Halfmann, Eckhard Hennig, Manfred Thole, and Tim Wichmann. *Analog Insydes - Release 2.1 Manual*. Fraunhofer-Institut für Techno- und Wirtschaftsmathematik, Kaiserslautern, Germany.

[19] Jiří Rohn. Systems of linear interval equations. *Linear Algebra and Its Applications*, 126:39–78, 1989.

[20] U. Tietze and Ch. Schenk. *Halbleiter-Schaltungstechnik*. Springer, 3rd edition, 1974.